

# S-wave ground state charmonium decays of $B_c$ mesons in the perturbative QCD approach

Zhou Rui<sup>a\*</sup> and Zhi-Tian Zou<sup>b</sup>

*a. School of Science, Hebei United University,*

*Tangshan 063009, Peoples Republic of China*

*b. Department of Physics, Yantai University, Yantai 264005, China*

(Dated: April 22, 2021)

## Abstract

We make a systematic investigation on the two-body nonleptonic decays  $B_c \rightarrow J/\Psi(\eta_c), M$  by employing the perturbative QCD approach based on  $k_T$  factorization, where  $M$  is a light pseudoscalar or vector or a heavy charmed meson. We predict the branching ratios and direct CP asymmetries of these  $B_c$  decays and also the transverse polarization fractions of  $B_c \rightarrow J/\Psi V, J/\psi D_{(s)}^*$  decays. It is found that these decays have a large branching ratios of the order of  $10^{-4} - 10^{-2}$  and could be measured by the future LHC-b experiment. Our predictions for the ratios of branching fractions  $\frac{\mathcal{BR}(B_c^+ \rightarrow J/\Psi D_s^+)}{\mathcal{BR}(B_c^+ \rightarrow J/\Psi \pi^+)}$ ,  $\frac{\mathcal{BR}(B_c^+ \rightarrow J/\Psi D_s^{*+})}{\mathcal{BR}(B_c^+ \rightarrow J/\Psi D_s^+)}$  and  $\frac{\mathcal{BR}(B_c^+ \rightarrow J/\Psi K^+)}{\mathcal{BR}(B_c^+ \rightarrow J/\Psi \pi^+)}$  are in good agreement with the data. A large transverse polarization fraction which can reach 48% is predicted in  $B_c^+ \rightarrow J/\Psi D_s^{*+}$  decay, which is consistent with the data. We find a possible direct CP violation in  $B_c \rightarrow J/\psi D^*$  decays, which are helpful to test the CP violating effects in  $B_c$  decays.

PACS numbers: 13.25.Hw, 12.38.Bx, 14.40.Nd

---

\*Electronic address: zhourui@heuu.edu.cn

## I. INTRODUCTION

Since the first discovery of the  $B_c$  meson by the CDF collaboration at Tevatron in 1998 through the semileptonic modes  $B_c \rightarrow J/\psi(\mu^+\mu^-)l^+X(l = e, \mu)$ [1], it has aroused a great deal of interest in studying  $B_c$  physics experimentally. Subsequent measurements of its mass and lifetime in different detectors via the two processes  $B_c^+ \rightarrow J/\psi l^+ \nu_l$  [2, 3] and  $B_c^+ \rightarrow J/\psi \pi^+$  [4, 5] have opened new windows for the analysis of the dynamics involved in the  $B_c$  decays. At the current level accuracy, around  $5 \times 10^{10}$   $B_c$  events are expected to be produced each year [6]. Up to now, the LHCb collaboration has measured the  $B_c$  mass with  $6273 \pm 1.3(stat) \pm 1.6(syst) \text{MeV}/c^2$  [7] and some new channels, such as  $B_c^+ \rightarrow J/\psi \pi^+ \pi^- \pi^+$  [8],  $B_c^+ \rightarrow J/\psi K^+$  [9],  $B_c^+ \rightarrow \psi(2S) \pi^+$  [10],  $B_c^+ \rightarrow J/\psi D_s^{(*)+}$  [11],  $B_c^+ \rightarrow J/\psi K^+ K^- \pi^+$  [12],  $B_c^+ \rightarrow B_s^0 \pi^+$  [13], and  $B_c^+ \rightarrow J/\psi 3\pi^+ 2\pi^-$  [14] for the first time. We can see all of the observed processes involving the  $J/\psi$  final state, due to the narrow peak of  $J/\psi$  and the high purity of  $J/\psi \rightarrow l^+ l^-$ , the decay modes containing the signal of  $J/\psi$  meson are among the most easily reconstructible  $B_c$  decay modes. One should expect that, in the following years, more and more charmonium decay modes of  $B_c$  meson will be measured with good precision in the LHCb experiments.

Compared with the  $B_{u,d,s}$  mesons, the  $B_c$  meson is of special interest. Being the ground state of two heavy quarks of different flavors ( $\bar{b}$  and  $c$ ),  $B_c$  decays via weak interaction only, while the strong and electromagnetic annihilation processes are forbidden. Since both of the two quarks are heavy, each of them can decay with the other as a spectator, the  $B_c$  meson have much shorter lifetime than other b-flavored mesons [15], pointing to the important role of the  $c$  quark in  $B_c$  decays. It has rich decay channels, and provides a very good place to study nonleptonic weak decays of heavy mesons, to test the standard model and to search for any new physics signals [16].

Theoretically, many hadronic  $B_c$  decay modes have been studied by various theoretical approaches. The perturbative QCD approach (pQCD)[17] is one of the recently developed theoretical tools based on QCD to deal with the nonleptonic  $B$  decays. Utilizing the  $k_T$  factorization instead of collinear factorization, this approach is free of end-point singularity. Thus the Feynman diagrams, including factorizable,

nonfactorizable, and annihilation type, are all calculable. Up to now, the pure annihilation type of charmless  $B_c \rightarrow PP, PV, VV, AV, AA, AP, SP, SV$  decays [18–24] and the charm decays of  $B_c \rightarrow D_{(s)}^{(*)}(P, V, T, D_{(s)}^{(*)})$  [25–29] have been studied systematically in the pQCD approach, where the term  $P, V, A, S, T$  refers to the pseudoscalar, vector, axial-vector, scalar and tensor charmless mesons, respectively.

In the present paper, we extend our pQCD analysis to the S-wave ground state charmonium decays of the  $B_c$  meson. The  $B_c \rightarrow J/\psi(\eta_c)\pi$  [30],  $B_c \rightarrow J/\psi K$  [31] decays have been studied in pQCD, compared to which the new ingredients of this paper are: (1) we updated the Cabibbo-Kobayashi-Maskawa (CKM) matrix elements and some input hadronic parameters according to the Particle Data Group 2012 [32]; (2) we have included the intrinsic  $b$  (the conjugate space coordinate of the parton transverse momentum  $k_T$ ) dependence for the  $B_c$  meson wave function, because it is observed that the intrinsic  $b$  dependence in the heavy meson wave functions is important [33]; (3) not only the  $B_c \rightarrow J/\psi(\eta_c), \pi(K)$  decays, but  $B_c \rightarrow (J/\psi, \eta_c)(\pi, K, K^*, \rho, D_{(s)}^{(*)})$  are investigated. In addition, a comprehensive study of these processes, which have been studied in the QCD coupling [34], the relativistic quark model [35], the covariant light-front quark model [38] and so on, is still lacking in pQCD. Our aim is to fill in this gap and provide a ready reference to the existing and forthcoming experiments to compare their data with the predictions in the pQCD approach. It will be shown that the obtained ratios of the branching ratios and polarization fractions are all in consistency with the existing data.

In the  $B_c$  rest frame, since both of the constituents ( $c, \bar{b}$ ) are heavy, they are almost at rest relative to each other. The  $B_c$  meson can be approximated as a nonrelativistic quarkonium system [36, 37]. In this sense the charm quark mass, which is considerably larger than the QCD scale, provides an intrinsic physical infrared regulator. The dynamics at this scale is still calculable perturbatively [36]. In the pQCD framework, since the spectator charm quark is almost at rest, a hard gluon is needed to transfer energy to make it a collinear quark into the final state meson. Meanwhile, the heavy charm mass will bring another expansion series of  $m_c/m_{B_c} \sim 0.2$ . In fact, the factorization theorem is applicable to the  $B_c$  system similar to the situation of the  $B$  meson [23] in the leading order of this expansion.

For the decays with a heavy charmonium and a light meson in the final states, since the emitted meson is a light meson, the factorization could be proved in the soft-collinear effective theory to all orders of the strong coupling constant in the heavy quark limit [38, 39]. For the decays with a heavy charmonium and a charm meson in the final states, both the charmonium and charm meson can emit from the weak vertex, which is similar to the double charm decays of the  $B_c$  meson [28]. The proof of factorization here is thus trivial. In fact, this type of process in  $B$  meson decays has been studied in the pQCD approach successfully [40].

Our paper is organized as follows: We review the pQCD factorization approach and then perform the perturbative calculations for these considered decay channels in Sec.II. The numerical results and discussions on the observables are given in Sec.III. The final section is devoted to our conclusions. Some details of related functions and the decay amplitudes are given in the Appendix.

## II. FRAMEWORK AND WAVE FUNCTION

At the quark level, the considered processes are characterized by the  $\bar{b} \rightarrow \bar{c}q\bar{q}'$  transition, with  $q = u, c$  and  $\bar{q}' = \bar{d}, \bar{s}$ . In the rest frame of the  $B_c$  meson, the spectator  $c$  quark is almost at rest due to the heavy mass. Therefore, a hard gluon is then needed to transform the  $c$  quark into a collinear object in the final charmonium or charmed meson. This makes the perturbative calculations into a six-quark interaction. These perturbative calculations meet end-point singularity in dealing with the meson distribution amplitudes at the end point. We take back the parton transverse momentum  $k_T$  to regulate this divergence. In the pQCD approach, the decay amplitude can be written as the following factorizing formula [41],

$$C(t) \otimes H(x, t) \otimes \Phi(x) \otimes \exp[-s(P, b) - 2 \int_{1/b}^t \frac{d\mu}{\mu} \gamma_q(\alpha_s(\mu))], \quad (1)$$

where  $C(t)$  is Wilson coefficient of the four-quark operator with the QCD radiative corrections.  $t$  is chosen as the largest energy scale in the hard part, in order to lower the largest logarithm. The term  $\exp[-s(P, b)]$  [42], the so-called Sudakov factor, results from summing up double logarithms caused by collinear divergence and soft divergence, with  $P$  denoting the dominant light-cone component of meson

momentum.  $\gamma_q = -\alpha_s/\pi$  is the quark anomalous dimension. The hard part  $H(x, t)$  can be perturbatively calculated including all possible Feynman diagrams without end-point singularity, such as factorizable, nonfactorizable and annihilation-type diagrams. The wave function  $\Phi(x)$ , which describes hadronization of the quark and antiquark to the meson, is not calculable and treated as nonperturbative inputs.

The meson wave function absorbs nonperturbative dynamics of the process, which is process independent. Using the wave functions determined from other well-measured processes, one can make quantitative predictions here. Similar to the situation of  $B$  meson, for  $B_c$  meson, one of the dominant Lorentz structure is considered in the numerical calculations, while the contribution induced by the other Lorentz structures is negligible [43]. In the nonrelativistic limit, we use the same distribution amplitude for  $B_c$  meson as those used in Refs. [27–29]

$$\Phi_{B_c}(x) = \frac{if_B}{4N_c} [(P + M_{B_c})\gamma_5\delta(x - \frac{m_c}{M_{B_c}})] \exp(-\frac{\omega_B^2 b^2}{2}), \quad (2)$$

in which the last exponent term represents the  $k_T$  dependence. The shape parameter  $\omega_B = 0.60 \pm 0.05$  GeV has been adopted in our previous analyses of the double charm decays of  $B_c$  meson [28].

The two-particle light-cone distribution amplitudes of the  $D_{(s)}/D_{(s)}^*$  meson can be written as [44]

$$\begin{aligned} \langle D_{(s)}(P_2) | q_\alpha(z) \bar{c}_\beta(0) | 0 \rangle &= \frac{i}{\sqrt{2N_c}} \int_0^1 dx e^{ixP_2 \cdot z} [\gamma_5 (P_2 + m_{D_{(s)}}) \phi_{D_{(s)}}(x, b)]_{\alpha\beta}, \\ \langle D_{(s)}^*(P_2) | q_\alpha(z) \bar{c}_\beta(0) | 0 \rangle &= -\frac{1}{\sqrt{2N_c}} \int_0^1 dx e^{ixP_2 \cdot z} [\not{e}_L (P_2 + m_{D_{(s)}^*}) \phi_{D_{(s)}^*}^L(x, b) \\ &\quad + \not{e}_T (P_2 + m_{D_{(s)}^*}) \phi_{D_{(s)}^*}^T(x, b)]_{\alpha\beta}, \end{aligned} \quad (3)$$

with the normalization conditions:

$$\int_0^1 dx \phi_{D_{(s)}}(x, 0) = \frac{f_{D_{(s)}}}{2\sqrt{2N_c}}, \quad \int_0^1 dx \phi_{D_{(s)}^*}^L(x, 0) = \int_0^1 dx \phi_{D_{(s)}^*}^T(x, 0) = \frac{f_{D_{(s)}^*}}{2\sqrt{2N_c}}. \quad (4)$$

Here we use  $f_{D_{(s)}^*} = f_{D_{(s)}^*}^T$  in the calculation. The value of  $f_{D_{(s)}^*}$  is determined by the following relations derived from HQET [45]:

$$f_{D_{(s)}^*} = \sqrt{\frac{m_{D_{(s)}}}{m_{D_{(s)}^*}}} f_{D_{(s)}}. \quad (5)$$

The distribution amplitude  $\phi_{D(s)^{(*)}}^{(L,T)}$  is taken as [46]

$$\phi_{D(s)^{(*)}}^{(L,T)} = \frac{3}{\sqrt{2N_c}} f_{D(s)^{(*)}} x(1-x)[1 + a_{D(s)^{(*)}}(1-2x)] \exp\left(-\frac{\omega_{D(s)^{(*)}}^2 b^2}{2}\right). \quad (6)$$

According to Ref. [47], we use  $a_D = 0.5 \pm 0.1, \omega_D = 0.1\text{GeV}$  for the  $D/D^*$  meson and  $a_{D_s} = 0.4 \pm 0.1, \omega_{D_s} = 0.2\text{GeV}$  for the  $D_s/D_s^*$  meson.

For the  $J/\psi(\eta_c)$  meson, in terms of the notation in Ref.[48], we decompose the nonlocal matrix elements for the longitudinally and transversely polarized  $J/\psi$  mesons and  $\eta_c$  into

$$\begin{aligned} \langle J/\psi(P, \epsilon^L) | \bar{c}(z)_\alpha c(0)_\beta | 0 \rangle &= \frac{1}{\sqrt{2N_c}} \int_0^1 dx e^{ixP \cdot z} [m_{J/\psi} \not{\epsilon}^L_{\alpha\beta} \psi^L(x, b) + (\not{\epsilon}^L P)_{\alpha\beta} \psi^t(x, b)], \\ \langle J/\psi(P, \epsilon^T) | \bar{c}(z)_\alpha c(0)_\beta | 0 \rangle &= \frac{1}{\sqrt{2N_c}} \int_0^1 dx e^{ixP \cdot z} [m_{J/\psi} \not{\epsilon}^T_{\alpha\beta} \psi^V(x, b) + (\not{\epsilon}^T P)_{\alpha\beta} \psi^T(x, b)], \\ \langle \eta_c(P) | \bar{c}(z)_\alpha c(0)_\beta | 0 \rangle &= -\frac{i}{\sqrt{2N_c}} \int_0^1 dx e^{ixP \cdot z} [(\gamma_5 P)_{\alpha\beta} \psi^v(x, b) + m_{\eta_c} (\gamma_5)_{\alpha\beta} \psi^s(x, b)], \end{aligned} \quad (7)$$

respectively.  $\psi^L, \psi^T$  and  $\psi^v$  denote for the twist-2 distribution amplitudes, while  $\psi^t, \psi^V$  and  $\psi^s$  for the twist-3 distribution amplitudes.  $x$  represents the momentum fraction of the charm quark inside the charmonium. In order to include the intrinsic  $b$  dependence for the  $J/\psi(\eta_c)$  meson wave function, we adopt the same model as [30]. For the wave functions of light vector and pseudoscalar mesons, the same form and parameters are adopted as [27] and one is referred to the original literature [49].

### A. $B_c \rightarrow (J/\psi, \eta_c)(P, V)$ decays

The effective Hamiltonian for these modes can be written as

$$\mathcal{H}_{eff} = \frac{G_F}{\sqrt{2}} V_{cb}^* V_{ud(s)} (C_1(\mu) O_1(\mu) + C_2(\mu) O_2(\mu)), \quad (8)$$

with  $V_{cb}^*$  and  $V_{ud(s)}$  the Cabibbo-Kobayashi-Maskawa (CKM) matrix elements,  $C_{1,2}(\mu)$  the perturbatively calculable Wilson coefficients, and  $O_{1,2}(\mu)$  the effective four-quark operators; their expressions are

$$\begin{aligned} O_1(\mu) &= \bar{b}_\alpha \gamma^\mu (1 - \gamma_5) c_\beta \otimes \bar{u}_\beta \gamma_\mu (1 - \gamma_5) q'_\alpha, \\ O_2(\mu) &= \bar{b}_\alpha \gamma^\mu (1 - \gamma_5) c_\alpha \otimes \bar{u}_\beta \gamma_\mu (1 - \gamma_5) q'_\beta, \end{aligned} \quad (9)$$

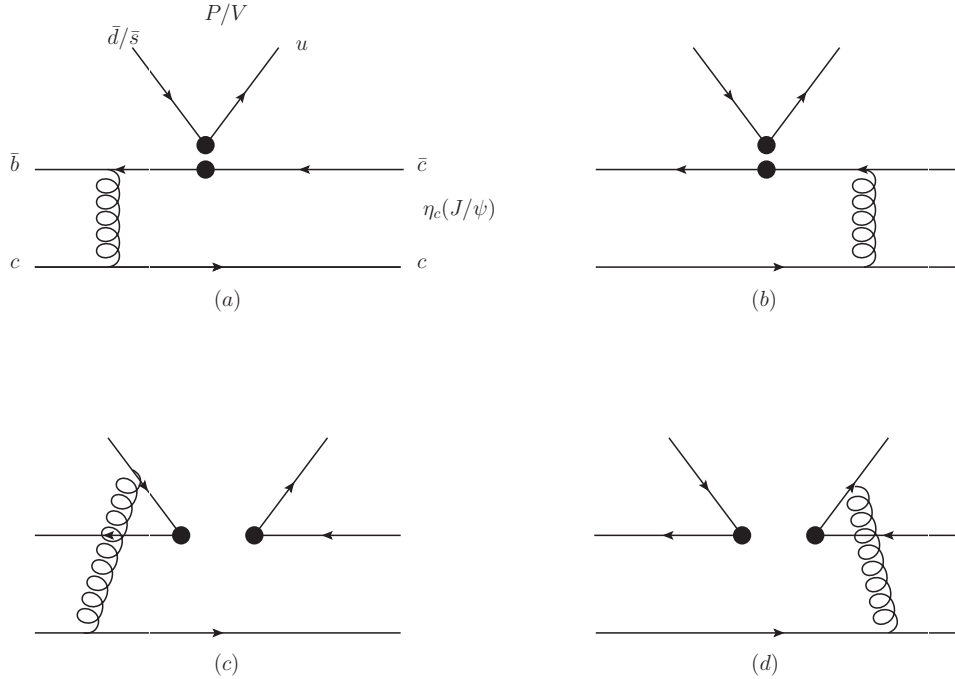


FIG. 1: Feynman diagrams for  $B_c \rightarrow (J/\psi, \eta_c)(P, V)$  decays.

where  $\alpha, \beta$  are color indices and the summation convention over repeated indices is understood. Since the four quarks in the operators are different from each other, there is no penguin contribution, and thus there is no  $CP$  violation. With the effective Hamiltonian given above, the Feynman diagrams corresponding to the concerned process are drawn in Fig.1 where the first two are of factorizable topology contributing to the form factor of  $B_c \rightarrow J/\psi(\eta_c)$ ; the last two diagrams are of nonfactorizable topology. With the meson wave functions, Sudakov factors and the six-quark hard subamplitude, after a straightforward calculation employing the pQCD formalism of Eq.1, we can get the explicit expressions of the amplitude in Fig.1, which are listed in Appendix A.

The total decay amplitude for the  $B_c \rightarrow (J/\psi, \eta_c)(P, V)$  can be given by

$$\mathcal{A}(B_c \rightarrow (J/\psi, \eta_c)(P, V)) = V_{cb}^* V_{ud(s)} [(C_2 + \frac{1}{3}C_1)\mathcal{F}_e + C_1\mathcal{M}_e]. \quad (10)$$

Here, the wilson coefficients  $C_{1,2}$  are actually convoluted with the amplitudes  $\mathcal{F}_e$  and  $\mathcal{M}_e$ . Note that the  $B_c \rightarrow J/\psi V$  decays contain more amplitudes associated with three different polarizations, one longitudinal and two transverse for the two

vector mesons, possible. The amplitude can be decomposed as

$$\mathcal{A} = \mathcal{A}^L + \mathcal{A}^N \epsilon_2^T \cdot \epsilon_3^T + i \mathcal{A}^T \epsilon_{\alpha\beta\rho\sigma} n^\alpha v^\beta \epsilon_2^{T\rho} \epsilon_3^{T\sigma}, \quad (11)$$

where  $\epsilon_2^T, \epsilon_3^T$  are the transverse polarization vectors for the two vector mesons, respectively.  $\mathcal{A}^L$  corresponds to the contributions of longitudinal polarization;  $\mathcal{A}^N$  and  $\mathcal{A}^T$  corresponds to the contributions of normal and transverse polarization, respectively, and the total amplitudes  $\mathcal{A}^{L,N,T}$  have the same structures as Eq.(10). The factorization formulas for the longitudinal, normal and transverse polarizations are all listed in Appendix AA.

### B. $B_c \rightarrow (J/\psi, \eta_c) D_{(s)}^{(*)}$ decays

The effective Hamiltonian for the flavor-changing  $b \rightarrow q'$  transition is given by

$$\mathcal{H}_{eff} = \frac{G_F}{\sqrt{2}} \{ (V_{cb}^* V_{cq'}) C_1(\mu) O_1(\mu) + C_2(\mu) O_2(\mu) - V_{tb}^* V_{tq'} \sum_{i=3}^{10} C_i(\mu) O_i(\mu) \} \quad (12)$$

with  $q' = d, s$ . The functions  $Q_i (i = 1, 2, \dots, 10)$  are the local four-quark operators:

#### 1. tree operators

$$\begin{aligned} O_1(\mu) &= \bar{b}_\alpha \gamma^\mu (1 - \gamma_5) c_\beta \otimes \bar{c}_\alpha \gamma_\mu (1 - \gamma_5) q'_\beta, \\ O_2(\mu) &= \bar{b}_\alpha \gamma^\mu (1 - \gamma_5) c_\alpha \otimes \bar{c}_\beta \gamma_\mu (1 - \gamma_5) q'_\beta, \end{aligned} \quad (13)$$

#### 2. QCD penguin operators

$$\begin{aligned} O_3(\mu) &= \bar{b}_\alpha \gamma^\mu (1 - \gamma_5) q'_\alpha \otimes \sum_q \bar{q}_\beta \gamma_\mu (1 - \gamma_5) q_\beta, \\ O_4(\mu) &= \bar{b}_\alpha \gamma^\mu (1 - \gamma_5) q'_\beta \otimes \sum_q \bar{q}_\alpha \gamma_\mu (1 - \gamma_5) q_\beta, \\ O_5(\mu) &= \bar{b}_\alpha \gamma^\mu (1 - \gamma_5) q'_\alpha \otimes \sum_q \bar{q}_\beta \gamma_\mu (1 + \gamma_5) q_\beta, \\ O_6(\mu) &= \bar{b}_\alpha \gamma^\mu (1 - \gamma_5) q'_\beta \otimes \sum_q \bar{q}_\alpha \gamma_\mu (1 + \gamma_5) q_\beta, \end{aligned} \quad (14)$$



### 3. electroweak penguin operators

$$\begin{aligned}
O_7(\mu) &= \frac{3}{2}\bar{b}_\alpha\gamma^\mu(1-\gamma_5)q'_\alpha \otimes \sum_q e_q\bar{q}_\beta\gamma_\mu(1+\gamma_5)q_\beta, \\
O_8(\mu) &= \frac{3}{2}\bar{b}_\alpha\gamma^\mu(1-\gamma_5)q'_\beta \otimes \sum_q e_q\bar{q}_\alpha\gamma_\mu(1+\gamma_5)q_\beta, \\
O_9(\mu) &= \frac{3}{2}\bar{b}_\alpha\gamma^\mu(1-\gamma_5)q'_\alpha \otimes \sum_q e_q\bar{q}_\beta\gamma_\mu(1-\gamma_5)q_\beta, \\
O_{10}(\mu) &= \frac{3}{2}\bar{b}_\alpha\gamma^\mu(1-\gamma_5)q'_\beta \otimes \sum_q e_q\bar{q}_\alpha\gamma_\mu(1-\gamma_5)q_\beta. \tag{15}
\end{aligned}$$

The sum over  $q$  runs over the quark fields that are active at the scale  $\mu = O(m_b)$ , i.e.  $q = (u, d, s, c, b)$ .

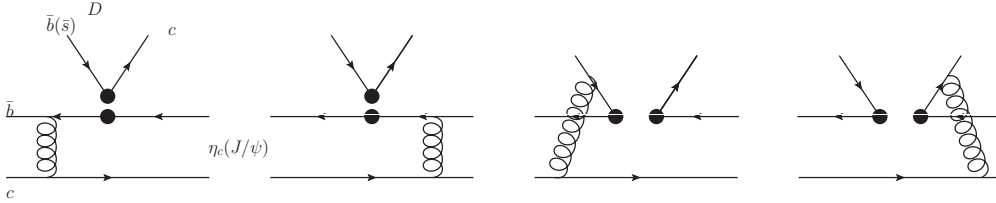


FIG. 2: Color-favored diagrams contributing to the Feynman diagrams for  $B_c \rightarrow (J/\psi, \eta_c)D_{(s)}^{(*)}$  decays.

There are 12 Feynman diagrams contributing to  $B_c \rightarrow (J/\psi, \eta_c)D_{(s)}^{(*)}$  decays at leading order. They involve three types: color-favored diagrams (we mark this kind of contribution with the subscript  $f$ ) shown in Fig.2, color-suppressed diagrams (marked with  $s$ ) shown in Fig.3 and annihilation diagrams (marked with  $a$ ) shown in Fig.4. Each type is classified into factorizable diagrams, where hard gluon connects

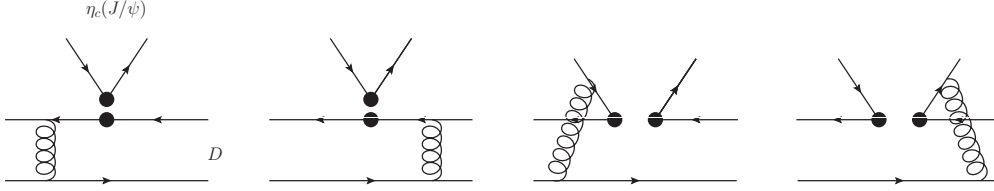


FIG. 3: Color-suppressed diagrams contributing to the Feynman diagrams for  $B_c \rightarrow (J/\psi, \eta_c)D_{(s)}^{(*)}$  decays.

the quarks in the same meson, and nonfactorizable diagrams, where hard gluon attaches the quarks in two different mesons. We also show the calculated formulas of each diagram for different channels in Appendix A A. The total decay amplitude for decay is given as

$$\begin{aligned}
\mathcal{A}(B_c \rightarrow (J/\psi, \eta_c)D_{(s)}^{(*)}) = & V_{cb}^*V_{cd}[(C_2 + \frac{1}{3}C_1)\mathcal{F}_f^{LL} + C_1\mathcal{M}_f^{LL} + \\
& (C_1 + \frac{1}{3}C_2)\mathcal{F}_s^{LL} + C_2\mathcal{M}_s^{LL} + (C_2 + \frac{1}{3}C_1)\mathcal{F}_a^{LL} + C_1\mathcal{M}_a^{LL}] \\
& -V_{tb}^*V_{td}[(C_4 + \frac{1}{3}C_3 + C_{10} + \frac{1}{3}C_9)\mathcal{F}_f^{LL} + (C_3 + C_9)\mathcal{M}_f^{LL} \\
& +(C_3 + \frac{1}{3}C_4 + C_9 + \frac{1}{3}C_{10})\mathcal{F}_s^{LL} + (C_4 + C_{10})\mathcal{M}_s^{LL} \\
& +(C_4 + \frac{1}{3}C_3 + C_{10} + \frac{1}{3}C_9)\mathcal{F}_a^{LL} + (C_3 + C_9)\mathcal{M}_a^{LL} \\
& +(C_6 + \frac{1}{3}C_5 + C_8 + \frac{1}{3}C_7)\mathcal{F}_f^{SP} + (C_6 + C_8)\mathcal{M}_s^{SP} \\
& +(C_5 + \frac{1}{3}C_6 + C_7 + \frac{1}{3}C_8)\mathcal{F}_s^{LR} + (C_5 + C_7)\mathcal{M}_f^{LR} \\
& +(C_6 + \frac{1}{3}C_5 + C_8 + \frac{1}{3}C_7)\mathcal{F}_a^{SP} + (C_5 + C_7)\mathcal{M}_a^{LR}]. \quad (16)
\end{aligned}$$

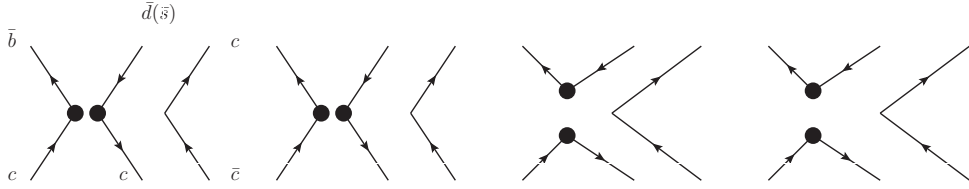


FIG. 4: Annihilation diagrams contributing to the Feynman diagrams for  $B_c \rightarrow (J/\psi, \eta_c) D_{(s)}^{(*)}$  decays.

Note that the amplitude  $\mathcal{F}_f^{SP}$  from the operators  $O_{5-8}$  vanishes when a vector meson ( $D_{(s)}^*$ ) is emitted from the weak vertex, because neither the scalar nor the pseudoscalar density gives contributions to the vector meson production, i.e.  $\langle D_{(s)}^* | S + P | 0 \rangle = 0$ .

### III. NUMERICAL RESULTS

We now use the method previously illustrated to estimate the physical observables (such as transition form factors, branching ratios, transverse polarization fractions and direct CP violations) of the considered  $B_c$  decays. For numerical calculation, some input parameters needed in the pQCD calculation are listed in Table I, while the input wave functions and various parameters of the light vector and pseudoscalar mesons are shown in the corresponding paper [27]. If not specified explicitly, we will take their central values as the default input.

TABLE I: The decay constants of mesons are from [28, 30], while other parameters are adopted in PDG [32] in our numerical calculation.

<b>Mass(GeV)</b>	$M_W = 80.399$	$M_{B_c} = 6.277$	$m_b = 4.2$	$m_c = 1.27$	$m_{J/\psi} = 3.097$
	$m_{\eta_c} = 2.981$	$m_D = 1.870$	$m_{D^*} = 2.010$	$m_{D_s} = 1.968$	$m_{D_s^*} = 2.112$
<b>CKM</b>	$ V_{cb}  = (40.9 \pm 1.1) \times 10^{-3}$	$ V_{ud}  = 0.97425 \pm 0.00022$	$ V_{us}  = 0.2252 \pm 0.0009$		
	$ V_{ub}  = (4.15 \pm 0.49) \times 10^{-3}$	$ V_{cd}  = 0.230 \pm 0.011$	$ V_{cs}  = 1.006 \pm 0.023$		
<b>Decay constants(MeV)</b>	$f_{B_c} = 489 \pm 4 \pm 3$	$f_{J/\psi} = 405 \pm 14$	$f_{\eta_c} = 420 \pm 50$		
	$f_D = 206.7 \pm 8.9$	$f_{D_s} = 257.5 \pm 6.1$			
<b>Lifetime</b>	$\tau_{B_c} = 0.453 \times 10^{-12}\text{s}$				

### A. $B_c \rightarrow \eta_c, J/\psi$ form factors

The diagrams (a) and (b) in Fig.1 give the contribution for  $B_c \rightarrow \eta_c, J/\psi$  transition form factor at the maximally recoiling point ( $q^2 = 0$ ). Our predictions of the form factors are collected in Table II compared with the results from other models. The first kind of uncertainties is from the uncertainty in the hadronic parameters:  $\omega_B = 0.60 \pm 0.05$  [28] for  $B_c$  meson and  $\omega = 0.60 \pm 0.1$  [30] for  $J/\psi(\eta_c)$  meson, while the second kind of uncertainties is from those in decay constants of the  $B_c$  meson and the charmonium meson, which are given in Table I. We find both  $A_0^{B_c \rightarrow J/\psi}$  and  $F_0^{B_c \rightarrow \eta_c}$  decrease with increasing shape parameters  $\omega_B$  and  $\omega$ . The former are more sensitive to the shape parameters than the decays constants, while the latter is just the reverse. Since the uncertainties from decay constant of  $\eta_c$  meson are large, the relevant uncertainties to  $F_0^{B_c \rightarrow \eta_c}$  are also large. We can see that the  $B_c \rightarrow \eta_c, J/\psi$  transition form factors are larger than those of  $B_c \rightarrow D_{(s)}^{(*)}$  in our previous study [28] under the perturbative QCD approach. As it is well known, compared with the  $D$  meson, the  $J/\psi(\eta_c)$  meson is heavier, and its velocity is lower in the rest frame of the  $B_c$  meson. The overlap between the initial and final state wave functions becomes larger, which certainly induces larger form factors.

The  $B_c \rightarrow J/\psi, \eta_c$  transition form factors have been widely studied in many theoretical frameworks, which are also collected in Table.II. Most of our results are found to be comparable to those of [30, 50–54], whereas the form factor  $A_0^{B_c \rightarrow J/\psi}$  in Ref. [53] is typically smaller, which can be discriminated by the future LHC

TABLE II: The form factors for  $F_0^{B_c \rightarrow \eta_c}$  and  $A_0^{B_c \rightarrow J/\psi}$  at  $q^2 = 0$  evaluated in the literature. The uncertainties are from the hadronic parameters and the decay constants, respectively. For comparison, we also cite the theoretical estimates of other models.

	This work	SDY[30] <sup>a</sup>	Kiselev [50]	IKP [51]	WSL [52]	HZ [53]	DSV [54]	EFG[35]
$F_0^{B_c \rightarrow \eta_c}$	$0.72^{+0.10+0.08}_{-0.08-0.09}$	$0.66 \sim 0.79$	0.66	0.76	0.61	0.87	0.58	0.47
$A_0^{B_c \rightarrow J/\psi}$	$0.64^{+0.08+0.02}_{-0.07-0.02}$	$0.65 \sim 0.77$	0.60	0.69	0.53	0.27	0.58	0.40

<sup>a</sup>We quote the result with the charmonium wave function for a harmonic-oscillator potential

TABLE III: Branching ratios ( $10^{-3}$ ) for  $B_c \rightarrow (J/\psi, \eta_c)(P, V)$ , together with results from other models. The errors for these entries correspond to the uncertainties in hadronic shape parameters, from the decay constants, and the scale dependence, respectively.

Channels	This work	[34]	[35]	[56]	[57]	[58]	[59]	[60]	[61]
$B_c^+ \rightarrow J/\psi K^+$	$0.19^{+0.04+0.02+0.02}_{-0.04-0.02-0.01}$	0.22	0.05	0.16	0.11	0.13	0.11	0.07	0.08
$B_c^+ \rightarrow J/\psi K^{*+}$	$0.48^{+0.09+0.04+0.05}_{-0.08-0.03-0.03}$	0.43	0.10	0.35	0.22	0.28	0.09	0.2	0.18
$B_c^+ \rightarrow \eta_c K^+$	$0.24^{+0.04+0.07+0.02}_{-0.05-0.06-0.01}$	0.38	0.07	0.17	0.13	0.15	0.03	0.02	0.11
$B_c^+ \rightarrow \eta_c K^{*+}$	$0.57^{+0.10+0.11+0.06}_{-0.08-0.09-0.03}$	0.77	0.11	0.31	0.20	0.25	0.06	0.04	0.18
$B_c^+ \rightarrow J/\psi \pi^+$	$2.33^{+0.63+0.16+0.48}_{-0.58-0.16-0.12}$	2.91	0.61	2.1	1.3	1.7	0.34	1.3	1.1
$B_c^+ \rightarrow J/\psi \rho^+$	$8.20^{+1.49+0.58+0.50}_{-1.28-0.56-0.62}$	8.08	1.6	6.5	4.0	4.9	1.8	3.7	3.1
$B_c^+ \rightarrow \eta_c \pi^+$	$2.98^{+0.84+0.75+0.52}_{-0.79-0.67-0.14}$	5.19	0.85	2.2	2.0	1.9	0.34	0.26	1.4
$B_c^+ \rightarrow \eta_c \rho^+$	$9.83^{+1.38+2.48+1.74}_{-1.29-2.20-0.47}$	14.5	2.1	5.9	4.2	4.5	1.06	0.67	3.3

experiments.

## B. Branching ratios

The branching ratios in the  $B_c$  meson rest frame can be written as

$$\mathcal{BR}(B_c \rightarrow (J/\psi, \eta_c)D_{(s)}^{(*)}) = \frac{G_F^2 \tau_{B_c}}{32\pi M_B} \sqrt{1 - (r_D - r_{J/\psi(\eta_c)})^2} \sqrt{1 - (r_D + r_{J/\psi(\eta_c)})^2} |\mathcal{A}|^2,$$

$$\mathcal{BR}(B_c \rightarrow (J/\psi, \eta_c)(P, V)) = \frac{G_F^2 \tau_{B_c}}{32\pi M_B} (1 - r_{J/\psi(\eta_c)}^2) |\mathcal{A}|^2, \quad (17)$$

where the mass ratios  $r_i$  and the decay amplitudes  $\mathcal{A}$  for each channel have been given explicitly in Appendix A. Our numerical results of branching ratios for  $B_c \rightarrow (J/\psi, \eta_c)(P, V)$  and  $B_c \rightarrow (J/\psi, \eta_c)D_{(s)}^{(*)}$  decays are listed in Tables III and Table

TABLE IV: Branching ratios ( $10^{-3}$ ) for  $B_c \rightarrow (J/\psi, \eta_c)D_s^{(*)}$ , together with results from other models. The errors for these entries correspond to the uncertainties in hadronic shape parameters, from the decay constants, and the scale dependence, respectively.

Channels	This work	[56]	[57]	[58]	[59]	[60]	[61]	[62]
$B_c^+ \rightarrow J/\psi D^+$	$0.28^{+0.04+0.02+0.06}_{-0.04-0.02-0.02}$	0.009	0.09	0.15	0.04	0.13	0.09	0.09
$B_c^+ \rightarrow J/\psi D^{*+}$	$0.67^{+0.11+0.05+0.15}_{-0.09-0.05-0.05}$	-	0.28	0.45	0.18	0.19	0.28	0.28
$B_c^+ \rightarrow \eta_c D^+$	$0.44^{+0.07+0.11+0.07}_{-0.06-0.09-0.03}$	0.012	0.15	0.19	0.06	0.05	0.14	0.10
$B_c^+ \rightarrow \eta_c D^{*+}$	$0.58^{+0.10+0.15+0.11}_{-0.08-0.13-0.04}$	0.010	0.10	0.19	0.07	0.02	0.13	0.10
$B_c^+ \rightarrow J/\psi D_s^+$	$8.05^{+1.39+0.57+1.66}_{-1.18-0.54-0.36}$	0.41	1.7	3.4	1.15	3.4	1.5	2.2
$B_c^+ \rightarrow J/\psi D_s^{*+}$	$20.45^{+4.35+1.44+4.50}_{-4.05-1.39-3.00}$	-	6.7	9.7	4.4	5.9	5.5	6.0
$B_c^+ \rightarrow \eta_c D_s^+$	$12.32^{+2.06+3.11+2.03}_{-1.79-2.76-1.01}$	0.54	2.8	4.4	1.79	5	2.6	2.5
$B_c^+ \rightarrow \eta_c D_s^{*+}$	$16.54^{+2.72+4.17+3.09}_{-2.34-3.70-1.70}$	0.44	2.7	3.7	1.49	0.38	2.4	2.0

IV, respectively. The first two errors are the same as for form factors in Table II, while the third error arises from the hard scale  $t$  varying from  $0.75t$  to  $1.25t$ , which characterizes the size of next-to-leading order (NLO) QCD contributions. We can see the branching ratios are sensitive to the choice of the hadronic parameters  $\omega_B$  and  $\omega$ , the combined uncertainties from them are about 20%. In addition, the uncertainties from the decay constants except for  $f_{\eta_c}$  are small. However, for  $B_c \rightarrow (J/\psi, \eta_c)D_s^{(*)}$  decays, the uncertainties from the hard scale  $t$  is large as shown in Table IV, which means the next-to-leading order contributions may be important for this decay mode. It reflects that the energy release in this type decay may be low for pQCD to play. The similar situation also exists in  $B_c \rightarrow BP, BV$  [55] and  $B \rightarrow (J/\psi, \eta_c)D^{(*)}$  [40] decays. In a recent paper [34], the authors have performed the  $B_c$  meson exclusive decays to S-wave charmonia and light pseudoscalar or vector mesons at the next-to-leading order (NLO) in the QCD coupling. The NLO corrections to  $B_c$  decays under the pQCD framework are still missing, thus beyond the scope of this paper. From Tables III and IV, we can see the former four processes have a relatively small branching ratio ( $10^{-4}$ ) owing to the CKM factor suppression, while the branching ratios of other processes are comparatively large ( $10^{-3} \sim 10^{-2}$ ) due to the CKM factor enhancement. The large branching ratio and the clear signals of the final states make their measurement easy at the LHCb experiments.

For comparison, we also cite other theoretical results [34, 35, 56–62] for the considered decays in Tables III and IV. In general, the results of the various model calculations are of the same order of magnitude for most channels, while our predictions are larger than those of other approaches. The difference may be due to at least two reasons: First, the calculations in Refs.[35, 56–62] use the same naive factorization approximation in which the form factors are important input parameters, smaller form factors always result in the smaller branching ratios. Second, in pQCD framework, the nonfactorizable contribution is considered, which is absent in traditional naive factorization. A constructive interference between the nonfactorizable contribution and the factorizable contribution will enhance our results. From Table III, we can see that our predicted branching ratios are comparable with [34] which also include the nonfactorizable contribution. Since the charmonium decays dominate the  $b \rightarrow c, u$  induced  $B_c$  decays, summing up all the branching ratios in Tables III and IV one obtains a total branching ratio of 10% which has to be compared with the 20% expected for the  $b \rightarrow c, u$  contribution to the total rate [16], this leaves plenty of room for the  $B_c$  meson to charmonium semileptonic, excited charmonium meson and nonresonant multibody decays.

The two decays  $B_c \rightarrow J/\psi\pi, J/\psi K$  have identical topology and similar kinematic properties, as shown in Fig. 1. In the limit of  $SU(3)$  flavor symmetry, the ratio of branching fractions  $\mathcal{BR}(B_c \rightarrow J/\psi K)/\mathcal{BR}(B_c \rightarrow J/\psi\pi)$  is dominated by the ratio of the relevant CKM matrix elements  $|V_{us}/V_{ud}|^2$ . After including the decay constants  $f_{K(\pi)}$ , the ratio is enhanced. With the input parameters in Table I, the expected ratio is 0.080, which is very close to our prediction 0.082. It means that the dominant contributions to the branching ratios come from the factorizable topology, while the nonfactorizable contribution is suppressed by the Wilson coefficient  $C_1$  (see Eq.10). Recently, the LHCb collaboration has measured this ratio to be  $0.069 \pm 0.019 \pm 0.005$  which is compatible with our pQCD prediction. For  $B_c \rightarrow \eta_c\pi, \eta_c K$  decays, our result of  $\mathcal{BR}(B_c \rightarrow \eta_c K)/\mathcal{BR}(B_c \rightarrow \eta_c\pi)$  is 0.081, which will be tested by the forthcoming experiments.

Due to  $m_{J/\psi} > m_{\eta_c}$  and the orbital angular momentum of the final states  $J/\psi M$  are larger than that of  $\eta_c M$ , the phase space for  $B_c \rightarrow J/\psi M$  decay is tighter than

that for  $B_c \rightarrow \eta_c M$  decay. Therefore, with the same input, the branching ratios for  $B_c \rightarrow J/\psi M$  and  $B_c \rightarrow \eta_c M$  decays have the following hierarchy

$$\mathcal{BR}(B_c \rightarrow J/\psi M) < \mathcal{BR}(B_c \rightarrow \eta_c M). \quad (18)$$

However, for  $B_c \rightarrow J/\psi D_{(s)}^*$  decays, the transverse polarization amplitude contributes to the branching ratio as large as the longitudinal polarization amplitude, which spoils the hierarchy relation in Eq.18.

It may be noted that the  $B_c \rightarrow (J/\psi, \eta_c) D_{(s)}^{(*)}$  decays involve contributions from the color-favored, color-suppressed and weak annihilation diagrams. It is expected that the color-favored factorizable amplitude  $\mathcal{F}_f^{LL}$  dominates in Eq.16. The color-suppressed nonfactorizable amplitude  $\mathcal{M}_s^{LL}$  and the annihilation amplitude  $\mathcal{F}_a^{LL}$ , are enhanced by the large Wilson coefficient  $C_2$  and  $C_2 + \frac{1}{3}C_1$ , respectively. However, the contribution from  $\mathcal{F}_a^{LL}$  are highly power suppressed due to a big cancellation between the first two factorizable annihilation diagrams in Fig. 4. Our numerical analysis shows that  $(C_2 + \frac{1}{3}C_1)\mathcal{F}_a^{LL}/(C_2 + \frac{1}{3}C_1)\mathcal{F}_f^{LL} \sim 1\%$  and  $C_2\mathcal{M}_s^{LL}/(C_2 + \frac{1}{3}C_1)\mathcal{F}_f^{LL} \sim 10\%$ . The interferences between  $\mathcal{F}_f^{LL}$  and  $\mathcal{M}_s^{LL}$  are constructive, while, the existing experimental data favor constructive interference in the  $B$  meson decays [63]. The predicted branching ratios of these modes would provide an interesting test of interference between the color-favored and color-suppressed  $B_c$  decays. Experimentally, the available measurements of the considered  $B_c$  decay are as follows [11]

$$\begin{aligned} \frac{\mathcal{BR}(B_c \rightarrow J/\psi D_s)}{\mathcal{BR}(B_c \rightarrow J/\psi \pi)} &= 2.90 \pm 0.57 \pm 0.24, \\ \frac{\mathcal{BR}(B_c \rightarrow J/\psi D_s^*)}{\mathcal{BR}(B_c \rightarrow J/\psi D_s)} &= 2.37 \pm 0.56 \pm 0.10, \end{aligned} \quad (19)$$

which is consistent with our predictions,

$$\begin{aligned} \frac{\mathcal{BR}(B_c \rightarrow J/\psi D_s)}{\mathcal{BR}(B_c \rightarrow J/\psi \pi)} &= 3.45_{-0.17}^{+0.49}, \\ \frac{\mathcal{BR}(B_c \rightarrow J/\psi D_s^*)}{\mathcal{BR}(B_c \rightarrow J/\psi D_s)} &= 2.54_{-0.21}^{+0.07}. \end{aligned} \quad (20)$$



### C. Transverse polarization fractions

For the  $B_c$  decays to two vector mesons, the decay amplitudes  $\mathcal{A}$  are defined in the helicity basis

$$\mathcal{A} = \sum_{i=0,+,-} |\mathcal{A}_i|^2, \quad (21)$$

where the helicity amplitudes  $\mathcal{A}_i$  have the following relationships with  $\mathcal{A}^{L,N,T}$

$$\mathcal{A}_0 = \mathcal{A}^L, \quad \mathcal{A}_\pm = \mathcal{A}^N \pm \mathcal{A}^T. \quad (22)$$

We also calculate the transverse polarization fractions  $\mathcal{R}_T$  of the  $B_c \rightarrow J/\psi(\rho, K^*, D_{(s)}^*)$  decays, with the definition given by

$$\mathcal{R}_T = \frac{|\mathcal{A}_+|^2 + |\mathcal{A}_-|^2}{|\mathcal{A}_0|^2 + |\mathcal{A}_+|^2 + |\mathcal{A}_-|^2}. \quad (23)$$

According to the power counting rules in the factorization assumption, the longitudinal polarization dominates the decay ratios and the transverse polarizations are suppressed [64] due to the helicity flips of the quark in the final state hadrons. Our predictions for the transverse polarization fractions of the tree-dominated  $B_c \rightarrow J/\psi V$  decays are given in Table V. These results have the following pattern

$$\mathcal{R}_T(J/\psi\rho) < \mathcal{R}_T(J/\psi K^*) < \mathcal{R}_T(J/\psi D^*) < \mathcal{R}_T(J/\psi D_s^*). \quad (24)$$

It can be simply understood by means of kinematics in the heavy-quark limit. The transverse polarization fractions  $\mathcal{R}_T$  of the  $B_c \rightarrow J/\psi(\rho, K^*, D^*, D_s^*)$  modes increase as the masses of the mesons  $\rho, K^*, D^*, D_s^*$  emitted from the weak vertex increase. This is similar to the case of  $B^0 \rightarrow (\rho^+, D^{*+}, D_s^{*+})D^{*-}$  and  $B^+ \rightarrow (\rho^+, D^{*+}, D_s^{*+})\rho^0$  [65]. From Table V, the modes  $B_c \rightarrow J/\psi(\rho, K^*)$  are indeed longitudinal polarization dominant, since the two transverse amplitudes are down by a power of  $r_{J/\psi}$  or  $r_v$  comparing with the longitudinal amplitudes. However, for  $B_c \rightarrow J/\psi D^*, J/\psi D_s^*$  decays, the transverse polarization fractions can reach 46% and 48%, respectively. Several reasons are given in order. First, the mass ratio  $r_D$  for  $D^*$  meson is about 2-3 times larger than the  $r_v$  for light vector meson, which enhances the color-favored transverse amplitude  $\mathcal{F}_f^{LL,T}$  and the normal amplitude  $\mathcal{F}_f^{LL,N}$ . Second, the annihilation contribution of operator  $O_6$  ( $\mathcal{F}_a^{SP,N(T)}$ ) is chirally enhanced in pQCD approach [66]. Third,

TABLE V: The transverse polarizations fractions (%) for  $B_c \rightarrow VV$ , together with results from RCQM [59]. The errors correspond to the combined uncertainty in the hadronic parameters, decay constants and the hard scale.

Channels	$B_c \rightarrow J/\psi\rho$	$B_c \rightarrow J/\psi K^*$	$B_c \rightarrow J/\psi D^*$	$B_c \rightarrow J/\psi D_s^*$
This work	$8^{+2}_{-1}$	$10^{+1}_{-1}$	$46^{+4}_{-3}$	$48^{+4}_{-4}$
RIQM [59]	7	10	41	43

the transverse polarization of the nonfactorizable color-suppressed diagrams in Figs. 3(c) and 3(d) does not encounter helicity flip suppression [28]. The combined effect above enhances the transverse polarization fractions of the  $B_c \rightarrow J/\psi D_{(s)}^*$  decays. Therefore, the above predictions on the transverse polarization fractions are reasonable in pQCD framework and comparable with the relativistic independent quark model (RIQM) [59]. The measurement of polarization fraction for  $B_c \rightarrow J/\psi D_s^*$  decay by the LHCb measurement [11] is

$$\mathcal{R}_T(J/\psi D_s^*) = (52 \pm 20)\%, \quad (25)$$

which is in good agreement with our result, while other predictions can be tested by the future data.

#### D. The direct CP asymmetries

Since there is only one kind of CKM phase involved in  $B_c$  decaying into charmonium and a light meson process, there should be no CP violation within the standard model. When the final states are charmonium and charmed meson, the CP asymmetries arise from the interference between the penguin diagrams and tree diagrams. The direct CP asymmetry  $A_{CP}^{dir}$  for a given mode can be written as

$$A_{CP}^{dir} = \frac{|\mathcal{A}|^2 - |\bar{\mathcal{A}}|^2}{|\mathcal{A}|^2 + |\bar{\mathcal{A}}|^2}, \quad (26)$$

where  $\bar{\mathcal{A}}$  is the charge conjugate decay amplitude of  $\mathcal{A}$ , which can be obtained by conjugating the CKM elements in  $\mathcal{A}$ . The direct CP asymmetry is tabulated in Table VI compared with the results from the Salpeter method [62]. Unlike the

TABLE VI: The direct CP asymmetry parameters ( $10^{-3}$ ) for  $B_c \rightarrow (J/\psi, \eta_c)D_{(s)}^{(*)}$ , together with results from the Salpeter method [62]. The errors arises from the hard scale  $t$ .

Final stats	$J/\psi D$	$J/\psi D^*$	$J/\psi D_s$	$J/\psi D_s^*$	$\eta_c D$	$\eta_c D^*$	$\eta_c D_s$	$\eta_c D_s^*$
This work	$1.5^{+0.6}_{-0.7}$	$12.7^{+4.0}_{-3.1}$	$0.1^{+0.1}_{-0.1}$	$0.7^{+0.2}_{-0.1}$	$-4.3^{+1.5}_{-2.0}$	$-2.4^{+0.2}_{-0.2}$	$-0.2^{+0.1}_{-0.1}$	$-0.1^{+0.03}_{-0.05}$
[62]	2.56	16.9	-0.151	-0.972	46.6	16.8	-2.69	-0.965

branching ratios, the direct CP asymmetry is not sensitive to the wave function parameters and CKM factors, since these parameter dependences canceled out in Eq. (26). In addition, the CKM angles ( $\gamma$ ) uncertainty is quite small ( $\sim 1\%$ ). Therefore, the theoretical error here is only referred to as the hard scale  $t$ . It can be seen our predictions on direct CP asymmetry parameters of  $B_c \rightarrow \eta_c D_{(s)}^{(*)}$  are negative, while the direct CP asymmetry parameter of the other modes is positive. The direct CP asymmetry parameters of the processes with a  $D$  meson in the final state are generally larger than those with a  $D_s$  meson, since in the former processes the penguin diagram contributions are enhanced by the ratio  $\frac{V_{tb}^* V_{td}}{V_{cb}^* V_{cd}} = 7.9$ , while in the latter processes,  $\frac{V_{tb}^* V_{ts}}{V_{cb}^* V_{cs}} = 0.9$ . However, the penguin amplitudes are still suppressed by the small Wilson coefficients from penguin operators in both of the two types of mode, our predictions on direct CP asymmetries are typically smaller in magnitude than [62]. From Tables IV and VI, it is easy to see that the decay  $B_c \rightarrow J/\psi D^*$  is helpful to test the CP violating effects due to its large branching ratio and CP asymmetry.

#### IV. CONCLUSION

In the pQCD framework, we have performed a systematic analysis of the two-body nonleptonic decays of the  $B_c$  meson with the final states involving one  $J/\psi(\eta_c)$  meson. Besides the color-favored emission diagrams, the nonfactorizable diagrams and the annihilation diagrams can also be evaluated in this approach. It is found that the predicted branching ratios range from  $10^{-4}$  up to  $10^{-2}$ , which are easily measured by the running LHCb in the near future. Our predictions for the ratios of branching fractions  $\frac{\mathcal{BR}(B_c^+ \rightarrow J/\Psi D_s^+)}{\mathcal{BR}(B_c^+ \rightarrow J/\Psi \pi^+)}$ ,  $\frac{\mathcal{BR}(B_c^+ \rightarrow J/\Psi D_s^{*+})}{\mathcal{BR}(B_c^+ \rightarrow J/\Psi D_s^+)}$  and  $\frac{\mathcal{BR}(B_c^+ \rightarrow J/\Psi K^+)}{\mathcal{BR}(B_c^+ \rightarrow J/\Psi \pi^+)}$  can explain

the data perfectly. We also have compared our results with the results of other studies. In general the results of the various model calculations are of the same order of magnitude while they can differ by factors of 10 for specific decay modes. In  $B_c$  decaying into one charmonium and one charmed meson process, the CP violation arises from the interference between the tree diagrams and the penguin diagrams. We found the direct CP asymmetries of  $B_c \rightarrow J/\psi D^*$  decays are somewhat large since the penguin diagrams contributions are enhanced by the CKM factor, which are helpful to test the CP violating effects. We also find that the transverse polarization contributions in  $B_c \rightarrow J/\psi D^*$ ,  $J/\psi D_s^*$  decays, which mainly come from the factorizable color-favored diagrams, the nonfactorizable color-suppressed diagrams and the chirally enhanced annihilation diagrams, are large.

We also discussed theoretical uncertainties arising from the hadronic parameters, decay constants and hard scale. The errors in Table III are dominant by the uncertainties from the hadronic parameters, while in Table IV, the uncertainties from the hard scale are as large as the hadronic parameters due to the included penguin diagram and annihilation diagram. Furthermore, the direct CP asymmetries in Table VI are very sensitive to the scale. These may suggest that further studies at the NLO level are required to improve the accuracy of the theoretical predictions on the charmonium decays of  $B_c$  meson.

### Acknowledgments

The authors are grateful to Cai-Dian Lü and Junfeng Sun for helpful discussions. This work is partially supported by National Natural Science Foundation of China under Grant No. 11347168 and No. 11347107, and Natural Science Foundation of Hebei Province of China, Grant No. A2014209308.

## Appendix A: the decay amplitudes

### 1. Factorization formulas for $B_c \rightarrow \eta_c \rho, \eta_c K^*$

The decay amplitude of factorizable diagrams in Figs.1(a) and (b) is

$$\begin{aligned} \mathcal{F}_e = & 2\sqrt{\frac{2}{3}}C_F f_B f_v \pi M_B^4 \sqrt{1 - r_{\eta_c}^2} \int_0^1 dx_2 \int_0^\infty b_1 b_2 db_1 db_2 \exp\left(-\frac{\omega_B^2 b_1^2}{2}\right) \\ & \{[\psi^s(x_2, b_2) (r_b - 2x_2) r_{\eta_c} + \psi^\nu(x_2, b_2) (x_2 - 2r_b)]E_{ab}(t_a)h(\alpha_e, \beta_a, b_1, b_2)S_t(x_2) \\ & - [\psi^\nu(x_2, b_2) (r_c + r_{\eta_c}^2) - 2\psi^s(x_2, b_2)r_{\eta_c}]E_{ab}(t_b)h(\alpha_e, \beta_b, b_2, b_1)S_t(x_1)]\}, \quad (\text{A1}) \end{aligned}$$

with  $r_i = m_i/M_B$  ( $i = b, c, \eta_c, J/\psi, D, v$ ) where  $m_i$  are the masses of quark or meson;  $C_F = 4/3$  is a color factor;  $f_v$  is the decay constant of the vector meson, emitted from the weak vertex. The factorization scales  $t_{a,b}$  are chosen as the maximal virtuality of internal particles in the hard amplitude. The function  $h$  and  $E_{ab}(t)$  are displayed in Appendix B. The factor  $S_t(x)$  is the jet function from the threshold resummation, whose definitions can be found in [25]. The terms proportional to  $r_D^2$  and  $r_c r_D$  have been neglected for small values.

The formula for nonfactorizable in diagrams Fig.1(c) and (d) is

$$\begin{aligned} \mathcal{M}_e = & -\frac{8}{3}C_F f_B \pi M_B^4 \sqrt{1 - r_{\eta_c}^2} \int_0^1 dx_2 dx_3 \int_0^\infty b_1 b_3 db_1 db_3 \phi_p^A(x_3) \exp\left(-\omega_B^2 \frac{b_1^2}{2}\right) \\ & \{[\psi^\nu(x_2, b_1) ((x_1 + 2x_2 + x_3 - 2) r_{\eta_c}^2 + x_1 - x_3) - (x_1 + x_2 - 1) \psi^s(x_2, b_1) r_{\eta_c}] \\ & E_{cd}(t_c)h(\beta_c, \alpha_e, b_3, b_1) + [(x_1 + x_2 - 1) \psi^s(x_2, b_1) r_{\eta_c} \\ & + \psi^\nu(x_2, b_1) ((x_3 - x_2) r_{\eta_c}^2 - 2x_1 - x_2 - x_3 + 2)]E_{cd}(t_d)h(\beta_d, \alpha_e, b_3, b_1)]\}. \quad (\text{A2}) \end{aligned}$$

where

$$\begin{aligned} \alpha_e &= [x_1 + r_{\eta_c}^2(x_2 - 1)][x_1 + x_2 - 1 + r_v^2(1 - x_2)]M_B^2, \\ \beta_a &= [r_b^2 + (1 + r_{\eta_c}^2(x_2 - 1))(x_2 - r_v^2(x_2 - 1))]M_B^2, \\ \beta_b &= [r_c^2 + (r_{\eta_c}^2 - x_1)(x_1 - 1 + r_v^2)]M_B^2, \\ \beta_c &= [x_1 + x_2 - 1 + r_v^2(1 - x_2 - x_3)][x_3 - x_1 - r_{\eta_c}^2(x_2 + x_3 - 1)]M_B^2, \\ \beta_d &= [x_1 + x_2 - 1 - r_v^2(x_2 - x_3)][1 - x_1 - x_3 - r_{\eta_c}^2(x_2 - x_3)]M_B^2. \quad (\text{A3}) \end{aligned}$$

The corresponding formula for  $B_c \rightarrow \eta_c \pi, \eta_c K$  is similar to Eqs.(A1) and (A2), but with the replacement  $f_v \rightarrow f_p, \phi_v \rightarrow \phi_p^A$ .

## 2. Factorization formulas for $B_c \rightarrow J/\psi\rho, J/\psi K^*$

We mark  $L$ ,  $N$  and  $T$  to denote the contributions from longitudinal polarization, normal polarization and transverse polarization, respectively:

$$\begin{aligned} \mathcal{F}_e^L = & 2\sqrt{\frac{2}{3}}C_F f_B f_v \pi M_B^4 \sqrt{1 - r_{J/\psi}^2} \int_0^1 dx_2 \int_0^\infty b_1 b_2 db_1 db_2 \exp\left(-\frac{\omega_B^2 b_1^2}{2}\right) \\ & \{[r_{J/\psi} \psi^t(x_2, b_2) (r_b - 2x_2) + \psi^L(x_2, b_2) (x_2 - 2r_b)] E_{ab}(t_a) h(\alpha_e, \beta_a, b_1, b_2) S_t(x_2)] \\ & - \psi^L(x_2, b_2) [r_{J/\psi}^2 + r_c] E_{ab}(t_b) h(\alpha_e, \beta_b, b_2, b_1) S_t(x_1)]\}, \end{aligned} \quad (\text{A4})$$

$$\begin{aligned} \mathcal{M}_e^L = & -\frac{8}{3}C_F f_B \pi M_B^4 \sqrt{1 - r_{J/\psi}^2} \int_0^1 dx_2 dx_3 \int_0^\infty b_1 b_3 db_1 db_3 \phi_p^A(x_3) \exp\left(-\omega_B^2 \frac{b_1^2}{2}\right) \times \\ & \{[\psi^L(x_2, b_1) (r_{J/\psi}^2 - 1) (x_1 - x_3) - r_{J/\psi} (x_1 + x_2 - 1) \psi^t(x_2, b_1)] \\ & E_{cd}(t_c) h(\beta_c, \alpha_e, b_3, b_1) + [r_{J/\psi} (x_1 + x_2 - 1) \psi^t(x_2, b_1) - \\ & \Psi^L(x_2, b_1) (r_{J/\psi}^2 (x_2 - x_3) + 2x_1 + x_2 + x_3 - 2)] E_{cd}(t_d) h(\beta_d, \alpha_e, b_3, b_1)]\} \end{aligned} \quad (\text{A5})$$

$$\begin{aligned} \mathcal{F}_e^N = & 2\sqrt{\frac{2}{3}}C_F f_B f_v \pi M_B^4 r_v \int_0^1 dx_2 \int_0^\infty b_1 b_2 db_1 db_2 \exp\left(-\frac{\omega_B^2 b_1^2}{2}\right) \\ & \{[r_{J/\psi} \psi^T(x_2, b_2) (-4r_b + x_2 + 1) + (r_b - 2) \psi^V(x_2, b_2)] E_{ab}(t_a) h(\alpha_e, \beta_a, b_1, b_2) S_t(x_2)] \\ & + \psi^T(x_2, b_2) [r_{J/\psi} (x_1 - 1)] E_{ab}(t_b) h(\alpha_e, \beta_b, b_2, b_1) S_t(x_1)]\}, \end{aligned} \quad (\text{A6})$$

$$\begin{aligned} \mathcal{F}_e^T = & -2\sqrt{\frac{2}{3}}C_F f_B f_v \pi M_B^4 r_v \int_0^1 dx_2 \int_0^\infty b_1 b_2 db_1 db_2 \exp\left(-\frac{\omega_B^2 b_1^2}{2}\right) \\ & \{[(r_b - 2) \psi^V(x_2, b_2) - r_{J/\psi} (x_2 - 1) \psi^T(x_2, b_2)] E_{ab}(t_a) h(\alpha_e, \beta_a, b_1, b_2) S_t(x_2)] \\ & - \psi^T(x_2, b_2) [r_{J/\psi} (x_1 - 1)] E_{ab}(t_b) h(\alpha_e, \beta_b, b_2, b_1) S_t(x_1)]\}, \end{aligned} \quad (\text{A7})$$

$$\begin{aligned} \mathcal{M}_e^N = & -\frac{8}{3}C_F f_B \pi M_B^4 r_v \int_0^1 dx_2 dx_3 \int_0^\infty b_1 b_3 db_1 db_3 \phi_v(x_3) \exp\left(-\omega_B^2 \frac{b_1^2}{2}\right) \times \\ & \{[2r_{J/\psi} (x_2 + x_3 - 1) \psi^T(x_2, b_1) \phi_V^a(x_3) + (x_3 - x_1) \psi^V(x_2, b_1) \phi_V^v(x_3)] \\ & E_{cd}(t_c) h(\beta_c, \alpha_e, b_3, b_1) - [2r_{J/\psi} \psi^T(x_2, b_1) ((x_2 - x_3) \phi_V^a(x_3) \\ & - (x_2 + x_3 - 2) \phi_V^v(x_3)) + (x_1 + x_3 - 1) \psi^V(x_2, b_1) (4\phi_V^a(x_3) + \phi_V^v(x_3))] \\ & E_{cd}(t_d) h(\beta_d, \alpha_e, b_3, b_1)]\}, \end{aligned} \quad (\text{A8})$$

$$\begin{aligned}
\mathcal{M}_e^T &= \frac{8}{3} C_F f_B \pi M_B^4 r_v \int_0^1 dx_2 dx_3 \int_0^\infty b_1 b_3 db_1 db_3 \phi_v(x_3) \exp(-\omega_B^2 \frac{b_1^2}{2}) \times \\
&\quad \{[2r_{J/\psi}(x_2 - x_3 - 1) \psi^T(x_2, b_1) \phi_V^a(x_3) + (x_3 - x_1) \psi^V(x_2, b_1) \phi_V^v(x_3)] \\
&\quad E_{cd}(t_c) h(\beta_c, \alpha_e, b_3, b_1) + [2r_{J/\psi} \psi^T(x_2, b_1) (x_2 - x_3) \phi_V^a(x_3) + \\
&\quad (x_1 + x_3 - 1) \psi^V(x_2, b_1) (4\phi_V^a(x_3) + \phi_V^v(x_3))] E_{cd}(t_d) h(\beta_d, \alpha_e, b_3, b_1)\} \quad (\text{A9})
\end{aligned}$$

where the expression of  $\beta_{a,b,c,d}$  and  $\alpha_e$  is the similar to that of Eq. (A3), but with the replacement  $r_{\eta_c} \rightarrow r_{J/\psi}$ . For  $B_c \rightarrow J/\psi\pi, J/\psi K$  decays, only the longitudinal polarization of  $J/\psi$  will contribute. We can obtain their amplitudes from the longitudinal polarization amplitudes for the  $B_c \rightarrow J/\psi\rho, J/\psi K^*$  decays with the replacement  $f_v \rightarrow f_p, \phi_v \rightarrow \phi_P^A$ .

### 3. Factorization formulas for $B_c \rightarrow \eta_c D_{(s)}$

We mark  $LL$ ,  $LR$ , and  $SP$  to denote the contributions from  $(V - A) \otimes (V - A)$ ,  $(V - A) \otimes (V + A)$  and  $(S - P) \otimes (S + P)$  operators, respectively:

$$\begin{aligned}
\mathcal{F}_f^{LL} &= 2\sqrt{\frac{2}{3(1-r_{\eta_c}^2)}} \pi M^4 f_B C_f f_D \int_0^1 dx_2 \int_0^\infty b_1 b_2 db_1 db_2 \exp(-\frac{\omega_B^2 b_1^2}{2}) \\
&\quad \{[\psi^s(x_2, b_2) (r_b - 2x_2) r_{\eta_c} + \psi^v(x_2, b_2) (2r_b - x_2) (r_{\eta_c}^2 - 1)] \\
&\quad E_{ab}(t_a) h(\alpha_e, \beta_a, b_1, b_2) S_t(x_2)] + [\psi^v(x_2, b_2) (r_{\eta_c}^2 + r_c) - 2\psi^s(x_2, b_2) r_{\eta_c}] \\
&\quad E_{ab}(t_b) h(\alpha_e, \beta_b, b_2, b_1) S_t(x_1)]\}, \quad (\text{A10})
\end{aligned}$$

$$\begin{aligned}
\mathcal{M}_f^{LL} &= \frac{8\pi M^4 f_B C_f}{3\sqrt{1-r_{\eta_c}^2}} \int_0^1 dx_2 dx_3 \int_0^\infty b_1 b_3 db_1 db_3 \phi_D(x_3, b_3) \exp(-\omega_B^2 \frac{b_1^2}{2}) \\
&\quad \{[\psi^s(x_2, b_1) r_{\eta_c} (r_c + x_2 - 1) + \psi^v(x_2, b_1) (x_3 - x_1 - 2(x_2 + x_3 - 1) r_{\eta_c}^2)] \\
&\quad E_{cd}(t_c) h(\beta_c, \alpha_e, b_3, b_1) + [-\psi^s(x_2, b_1) r_{\eta_c} (r_c + x_2 - 1) + \psi^v(x_2, b_1) \\
&\quad (-2(x_3 - 1) r_{\eta_c}^2 + 2r_c + x_2 + x_3 - 2)] E_{cd}(t_d) h(\beta_d, \alpha_e, b_3, b_1)]\}, \quad (\text{A11})
\end{aligned}$$

$$\begin{aligned}
\mathcal{F}_a^{LL} &= 8\pi M^4 f_B C_f \int_0^1 dx_2 dx_3 \int_0^\infty b_2 b_3 db_2 db_3 \phi_D(x_3, b_3) \\
&\quad \{[\psi^v(x_2, b_2) ((2x_3 - 1) r_{\eta_c}^2 - x_3 + 1) - 2r_{\eta_c} (r_c + (x_3 - 2) r_D) \psi^s(x_2, b_2)] \\
&\quad E_{ef}(t_e) h(\alpha_a, \beta_e, b_2, b_3) - [2(x_2 + 1) r_D \psi^s(x_2, b_2) r_{\eta_c} - x_2 \psi^v(x_2, b_2) (r_{\eta_c}^2 - 1)] \\
&\quad E_{ef}(t_f) h(\alpha_a, \beta_f, b_3, b_2)]\}, \quad (\text{A12})
\end{aligned}$$

$$\begin{aligned}
\mathcal{M}_a^{LL} &= \frac{8}{3}\pi M^4 f_B C_f \int_0^1 dx_2 dx_3 \int_0^\infty b_1 b_2 db_1 db_2 \phi_D(x_3, b_2) \exp(-\omega_B^2 \frac{b_1^2}{2}) \\
&\quad \{[x_2 \psi^v(x_2, b_2) + r_D r_{\eta_c} (x_2 - x_3 + 1) \psi^s(x_2, b_2)] E_{gh}(t_g) h(\beta_g, \alpha_a, b_1, b_2) \\
&\quad + [(r_b (r_{\eta_c}^2 - 1) - 2(x_2 + x_3 - 1) r_{\eta_c}^2 - x_1 + x_3) \psi^v(x_2, b_2) \\
&\quad - (4r_b + x_2 - x_3 - 1) r_D r_{\eta_c} \psi^s(x_2, b_2)] E_{gh}(t_h) h(\beta_h, \alpha_a, b_1, b_2)\}, \quad (A13)
\end{aligned}$$

$$\begin{aligned}
\mathcal{F}_s^{LL} &= \mathcal{F}_s^{LR} = -2\sqrt{\frac{2}{3}}\pi M^4 f_B C_f f_{\eta_c} \int_0^1 dx_2 \int_0^\infty b_1 b_2 db_1 db_2 \phi_D(x_2, b_2) \exp(-\frac{\omega_B^2 b_1^2}{2}) \\
&\quad \{[(2r_b - 2x_2 + 1) r_{\eta_c}^2 + r_D (r_b - 2x_2) - 2r_b + x_2] E_{ab}(t_{as}) h(\alpha_{es}, \beta_{as}, b_1, b_2) \\
&\quad S_t(x_2) + (r_c - 2r_D) E_{ab}(t_{bs}) h(\alpha_{es}, \beta_{bs}, b_2, b_1) S_t(x_1)\}, \quad (A14)
\end{aligned}$$

$$\begin{aligned}
\mathcal{M}_s^{LL} &= \frac{8}{3}\pi M^4 f_B C_f \int_0^1 dx_2 dx_3 \int_0^\infty b_1 b_3 db_1 db_3 \phi_D(x_2, b_1) \psi^v(x_3, b_3) \exp(-\omega_B^2 \frac{b_1^2}{2}) \\
&\quad \{[(x_2 - 1) r_D + x_3 - x_1] E_{cd}(t_{cs}) h(\beta_{cs}, \alpha_{es}, b_3, b_1) \\
&\quad + [-2(x_2 - 1) r_{\eta_c}^2 + 2r_c - (x_2 - 1) r_D + x_2 + x_3 - 2] \\
&\quad E_{cd}(t_{ds}) h(\beta_{ds}, \alpha_{es}, b_3, b_1)\}, \quad (A15)
\end{aligned}$$

$$\begin{aligned}
\mathcal{M}_f^{LR} &= \frac{8}{3}\pi M^4 f_B C_f r_D \int_0^1 dx_2 dx_3 \int_0^\infty b_1 b_3 db_1 db_3 \phi_D(x_3, b_3) \exp(-\omega_B^2 \frac{b_1^2}{2}) \times \\
&\quad \{[-(x_2 - x_3 - 1) \psi^s(x_2, b_1) r_{\eta_c} + x_3 \psi^v(x_2, b_1)] E_{cd}(t_c) h(\beta_c, \alpha_e, b_3, b_1) \\
&\quad + [\psi^s(x_2, b_1) r_{\eta_c} (r_c - (x_3 + x_2 - 2) r_D) + \psi^v(x_2, b_1) (-r_c + (x_3 - 1) r_D)] \\
&\quad E_{cd}(t_d) h(\beta_d, \alpha_e, b_3, b_1)\}. \quad (A16)
\end{aligned}$$

$$\begin{aligned}
\mathcal{M}_a^{LR} &= -\frac{8}{3}\pi M^4 f_B C_f \int_0^1 dx_2 dx_3 \int_0^\infty b_1 b_2 db_1 db_2 \phi_D(x_3, b_2) \exp(-\omega_B^2 \frac{b_1^2}{2}) \times \\
&\quad \{[(x_3 - 1) r_D \psi^v(x_2, b_2) - \psi^s(x_2, b_2) r_{\eta_c} (2r_c - x_2)] E_{gh}(t_g) h(\beta_g, \alpha_a, b_1, b_2) \\
&\quad - [r_D (r_b + x_3) \psi^v(x_2, b_2) - \psi^s(x_2, b_2) r_{\eta_c} (r_b - r_c - x_2 + 1)] \\
&\quad E_{gh}(t_h) h(\beta_h, \alpha_a, b_1, b_2)\}. \quad (A17)
\end{aligned}$$

$$\begin{aligned}
\mathcal{M}_s^{SP} &= \frac{8\pi M^4 f_B C_f}{3\sqrt{1 - r_{\eta_c}^2}} \int_0^1 dx_2 dx_3 \int_0^\infty b_1 b_3 db_1 db_3 \phi_D(x_2, b_1) \exp(-\omega_B^2 \frac{b_1^2}{2}) \times \\
&\quad \{\psi^v(x_3, b_3) [-(x_2 - 1) (2r_{\eta_c}^2 + r_D - 1) + 2r_c - x_3] \\
&\quad E_{cd}(t_{cs}) h(\beta_{cs}, \alpha_{es}, b_3, b_1) - [r_c \psi^s(x_3, b_3) r_{\eta_c} + \psi^v(x_3, b_3) \\
&\quad (- (x_2 - 1) r_D + x_1 + x_3 - 1)] E_{cd}(t_{ds}) h(\beta_{ds}, \alpha_{es}, b_3, b_1)\}, \quad (A18)
\end{aligned}$$



$$\begin{aligned}
\mathcal{F}_a^{SP} = & -\frac{16\pi M^4 f_B C_f}{\sqrt{1-r_{\eta_c}^2}} \int_0^1 dx_2 dx_3 \int_0^\infty b_2 b_3 db_2 db_3 \phi_D(x_3, b_3) \times \\
& \{[\psi^v(x_2, b_2)(r_c + (x_3 - 1)r_D) - 2\psi^s(x_2, b_2)r_{\eta_c}]E_{ef}(t_e)h(\alpha_a, \beta_e, b_2, b_3) \\
& - [x_2 r_{\eta_c} \psi^s(x_2, b_2) + 2r_D \psi^v(x_2, b_2)]E_{ef}(t_f)h(\alpha_a, \beta_f, b_3, b_2)\}, \tag{A19}
\end{aligned}$$

$$\begin{aligned}
\mathcal{F}_f^{SP} = & -4\sqrt{\frac{2}{3}}\pi M^4 f_B C_f f_D r_D \int_0^1 dx_2 \int_0^\infty b_1 b_2 db_1 db_2 \exp(-\frac{\omega_B^2 b_1^2}{2}) \\
& \{[(r_b - 2)\psi^v(x_2, b_2) - \psi^s(x_2, b_2)(4r_b - x_2 - 1)r_{\eta_c}] \\
& E_{ab}(t_a)h(\alpha_e, \beta_a, b_1, b_2)S_t(x_2)] - 2\psi^s(x_2, b_2)r_{\eta_c} \\
& E_{ab}(t_b)h(\alpha_e, \beta_b, b_2, b_1)S_t(x_1)\}, \tag{A20}
\end{aligned}$$

where

$$\begin{aligned}
\alpha_e &= -[x_1 + r_{\eta_c}^2(x_2 - 1)][x_1 + x_2 - 1 + (1 - x_2)r_D^2]M_B^2, \\
\alpha_{es} &= -[x_1 + r_D^2(x_2 - 1)][x_1 + x_2 - 1 + (1 - x_2)r_{\eta_c}^2]M_B^2, \\
\beta_a &= [r_b^2 - (1 + r_{\eta_c}^2(x_2 - 1))(x_2 - r_D^2(x_2 - 1))]M_B^2, \\
\beta_b &= [r_c^2 + (r_{\eta_c}^2 - x_1)(r_D^2 + x_1 - 1)]M_B^2, \\
\beta_c &= -[x_1 + x_2 - 1 + (1 - x_2 - x_3)r_D^2][r_{\eta_c}^2(x_2 + x_3 - 1) - x_3 + x_1]M_B^2, \\
\beta_d &= r_c^2 M_B^2 - [x_1 + x_2 - 1 - (x_2 - x_3)r_D^2][x_1 + x_3 - 1 + r_{\eta_c}^2(x_2 - x_3)]M_B^2, \\
\beta_{as} &= [r_b^2 - (1 + r_D^2(x_2 - 1))(x_2 - r_{\eta_c}^2(x_2 - 1))]M_B^2, \\
\beta_{bs} &= [(r_D^2 - x_1)(r_{\eta_c}^2 + x_1 - 1)]M_B^2, \\
\beta_{cs} &= r_c^2 M_B^2 - [x_1 + x_2 - 1 + (1 - x_2 - x_3)r_{\eta_c}^2][r_D^2(x_2 + x_3 - 1) - x_3 + x_1]M_B^2, \\
\beta_{ds} &= r_c^2 M_B^2 - [x_1 + x_2 - 1 - (x_2 - x_3)r_{\eta_c}^2][x_1 + x_3 - 1 + r_D^2(x_2 - x_3)]M_B^2, \\
\alpha_a &= -[1 - x_3 + r_{\eta_c}^2(x_2 + x_3 - 1)][x_2 - r_D^2(x_2 + x_3 - 1)]M_B^2, \\
\beta_e &= [r_c^2 - (1 + (r_{\eta_c}^2 - 1)x_3)(1 - r_D^2 x_3)]M_B^2, \\
\beta_f &= [1 + r_{\eta_c}^2(x_2 - 1)][x_2 - r_D^2(x_2 - 1)]M_B^2, \\
\beta_g &= r_c^2 M_B^2 - (r_{\eta_c}^2(1 - x_3 - x_2) + x_1 + x_3 - 1)(r_D^2(x_2 + x_3 - 1) + x_1 - x_2)M_B^2, \\
\beta_h &= r_b^2 M_B^2 - (r_{\eta_c}^2(x_2 + x_3 - 1) - x_3 + x_1)(r_D^2(1 - x_2 - x_3) + x_1 + x_2 - 1)M_B^2. \tag{A21}
\end{aligned}$$

#### 4. Factorization formulas for $B_c \rightarrow \eta_c D_{(s)}^*$

$$\begin{aligned}
\mathcal{F}_f^{LL} &= 2\sqrt{\frac{2}{3(1-r_{\eta_c}^2)}}\pi M^4 f_B C_f f_D \int_0^1 dx_2 \int_0^\infty b_1 b_2 db_1 db_2 \exp\left(-\frac{\omega_B^2 b_1^2}{2}\right) \\
&\quad \{[\psi^s(x_2, b_2)(r_b - 2x_2)r_{\eta_c} + \psi^v(x_2, b_2)(2r_b - x_2)(r_{\eta_c}^2 - 1)] \\
&\quad E_{ab}(t_a)h(\alpha_e, \beta_a, b_1, b_2)S_t(x_2)] + [\psi^v(x_2, b_2)(r_{\eta_c}^2 + r_c) - 2\psi^s(x_2, b_2)r_{\eta_c}] \\
&\quad E_{ab}(t_b)h(\alpha_e, \beta_b, b_2, b_1)S_t(x_1)]\}, \tag{A22}
\end{aligned}$$

$$\begin{aligned}
\mathcal{M}_f^{LL} &= \frac{8\pi M^4 f_B C_f}{3\sqrt{1-r_{\eta_c}^2}} \int_0^1 dx_2 dx_3 \int_0^\infty b_1 b_3 db_1 db_3 \phi_D(x_3, b_3) \exp\left(-\omega_B^2 \frac{b_1^2}{2}\right) \\
&\quad \{[\psi^s(x_2, b_1)r_{\eta_c}(r_c + x_2 - 1) + \psi^v(x_2, b_1)(x_3 - x_1 - 2(x_2 + x_3 - 1)r_{\eta_c}^2)] \\
&\quad E_{cd}(t_c)h(\beta_c, \alpha_e, b_3, b_1) + [-\psi^s(x_2, b_1)r_{\eta_c}(r_c + x_2 - 1) + \psi^v(x_2, b_1) \\
&\quad (-2(x_2 + x_3 - 1)r_{\eta_c}^2 + 2r_c + x_2 + x_3 - 2)]E_{cd}(t_d)h(\beta_d, \alpha_e, b_3, b_1)]\}, \tag{A23}
\end{aligned}$$

$$\begin{aligned}
\mathcal{F}_a^{LL} &= \frac{8\pi M^4 f_B C_f}{\sqrt{1-r_{\eta_c}^2}} \int_0^1 dx_2 dx_3 \int_0^\infty b_2 b_3 db_2 db_3 \phi_D(x_3, b_3) \\
&\quad \{[\psi^v(x_2, b_2)((2x_3 - 1)r_{\eta_c}^2 - x_3 + 1) - 2r_{\eta_c}(r_c + x_3 r_D)\psi^s(x_2, b_2)]E_{ef}(t_e) \\
&\quad h(\alpha_a, \beta_e, b_2, b_3) - x_2 \psi^v(x_2, b_2)(1 - r_{\eta_c}^2)E_{ef}(t_f)h(\alpha_a, \beta_f, b_3, b_2)]\}, \tag{A24}
\end{aligned}$$

$$\begin{aligned}
\mathcal{M}_a^{LL} &= \frac{8\pi M^4 f_B C_f}{3\sqrt{1-r_{\eta_c}^2}} \int_0^1 dx_2 dx_3 \int_0^\infty b_1 b_2 db_1 db_2 \phi_D(x_3, b_2) \exp\left(-\omega_B^2 \frac{b_1^2}{2}\right) \\
&\quad \{[x_2 \psi^v(x_2, b_2) + r_D r_{\eta_c}(x_2 + x_3 - 1)\psi^s(x_2, b_2)]E_{gh}(t_g)h(\beta_g, \alpha_a, b_1, b_2) \\
&\quad - [(r_b(r_{\eta_c}^2 - 1) - 2(x_2 + x_3 - 1)r_{\eta_c}^2 + x_3 - x_1)\psi^v(x_2, b_2) \\
&\quad + (x_2 + x_3 - 1)r_D r_{\eta_c} \psi^s(x_2, b_2)]E_{gh}(t_h)h(\beta_h, \alpha_a, b_1, b_2)]\}, \tag{A25}
\end{aligned}$$

$$\begin{aligned}
\mathcal{F}_s^{LL} = \mathcal{F}_s^{LR} &= -2\sqrt{\frac{2}{3(1-r_{\eta_c}^2)}}\pi M^4 f_B C_f f_{\eta_c} \int_0^1 dx_2 \int_0^\infty b_1 b_2 db_1 db_2 \phi_D(x_2, b_2) \exp\left(-\frac{\omega_B^2 b_1^2}{2}\right) \\
&\quad \{[(2r_b - 2x_2 + 1)r_{\eta_c}^2 + r_D(r_b - 2x_2) - 2r_b + x_2] \\
&\quad E_{ab}(t_{as})h(\alpha_{es}, \beta_{as}, b_1, b_2)S_t(x_2) - r_c E_{ab}(t_{bs})h(\alpha_{es}, \beta_{bs}, b_2, b_1)S_t(x_1)]\}, \tag{A26}
\end{aligned}$$

$$\begin{aligned}
\mathcal{M}_s^{LL} &= -\frac{8\pi M^4 f_B C_f}{3\sqrt{1-r_{\eta_c}^2}} \int_0^1 dx_2 dx_3 \int_0^\infty b_1 b_3 db_1 db_3 \phi_D(x_2, b_1) \psi^v(x_3, b_3) \exp\left(-\omega_B^2 \frac{b_1^2}{2}\right) \\
&\quad \{[(x_2 - 1)r_D - x_3 + x_1]E_{cd}(t_{cs})h(\beta_{cs}, \alpha_{es}, b_3, b_1) \\
&\quad - [-2(x_2 - 1)r_{\eta_c}^2 + 2r_c - (x_2 - 1)r_D + x_2 + x_3 - 2] \\
&\quad E_{cd}(t_{ds})h(\beta_{ds}, \alpha_{es}, b_3, b_1)]\}, \tag{A27}
\end{aligned}$$

$$\begin{aligned}
\mathcal{M}_f^{LR} = & \frac{8\pi M^4 f_B C_f r_D}{3\sqrt{1-r_{\eta_c}^2}} \int_0^1 dx_2 dx_3 \int_0^\infty b_1 b_3 db_1 db_3 \phi_D(x_3, b_3) \exp(-\omega_B^2 \frac{b_1^2}{2}) \times \\
& \{[(x_2 + x_3 - 1) \psi^s(x_2, b_1) r_{\eta_c} + x_3 \psi^v(x_2, b_1)] E_{cd}(t_c) h(\beta_c, \alpha_e, b_3, b_1) \\
& - [\psi^s(x_2, b_1) r_{\eta_c} (r_c + (x_3 - x_2) r_D) + \psi^v(x_2, b_1) (r_c + (x_3 - 1) r_D)] \\
& E_{cd}(t_d) h(\beta_d, \alpha_e, b_3, b_1)\}. \tag{A28}
\end{aligned}$$

$$\begin{aligned}
\mathcal{M}_a^{LR} = & -\frac{8\pi M^4 f_B C_f}{3\sqrt{1-r_{\eta_c}^2}} \int_0^1 dx_2 dx_3 \int_0^\infty b_1 b_2 db_1 db_2 \phi_D(x_3, b_2) \exp(-\omega_B^2 \frac{b_1^2}{2}) \times \\
& \{[(x_3 - 1) r_D \psi^v(x_2, b_2) - \psi^s(x_2, b_2) r_{\eta_c} (2r_c - x_2)] E_{gh}(t_g) h(\beta_g, \alpha_a, b_1, b_2) \\
& - [r_D (r_b + x_3) \psi^v(x_2, b_2) - \psi^s(x_2, b_2) r_{\eta_c} (r_b - r_c - x_2 + 1)] \\
& E_{gh}(t_h) h(\beta_h, \alpha_a, b_1, b_2)\}. \tag{A29}
\end{aligned}$$

$$\begin{aligned}
\mathcal{M}_s^{SP} = & \frac{8\pi M^4 f_B C_f}{3\sqrt{1-r_{\eta_c}^2}} \int_0^1 dx_2 dx_3 \int_0^\infty b_1 b_3 db_1 db_3 \phi_D(x_2, b_1) \exp(-\omega_B^2 \frac{b_1^2}{2}) \times \\
& \{\psi^v(x_3, b_3) [-(x_2 - 1) (2r_{\eta_c}^2 + r_D - 1) + 2r_c - x_3] \\
& E_{cd}(t_{cs}) h(\beta_{cs}, \alpha_{es}, b_3, b_1) - [r_c \psi^s(x_3, b_3) r_{\eta_c} + \psi^v(x_3, b_3) \\
& ((x_2 - 1) r_D + x_1 + x_3 - 1)] E_{cd}(t_{ds}) h(\beta_{ds}, \alpha_{es}, b_3, b_1)\}, \tag{A30}
\end{aligned}$$

$$\begin{aligned}
\mathcal{F}_a^{SP} = & -\frac{16\pi M^4 f_B C_f}{\sqrt{1-r_{\eta_c}^2}} \int_0^1 dx_2 dx_3 \int_0^\infty b_2 b_3 db_2 db_3 \phi_D(x_3, b_3) \times \\
& \{[\psi^v(x_2, b_2) (r_c - (x_3 - 1) r_D) - 2\psi^s(x_2, b_2) r_{\eta_c}] \\
& E_{ef}(t_e) h(\alpha_a, \beta_e, b_2, b_3) - x_2 r_{\eta_c} \psi^s(x_2, b_2) E_{ef}(t_f) h(\alpha_a, \beta_f, b_3, b_2)\}, \tag{A31}
\end{aligned}$$

where the expressions of  $\beta$  and  $\alpha$  are the same as those of Eq. (A21).

## 5. Factorization formulas for $B_c \rightarrow J/\Psi D_{(s)}$

$$\begin{aligned}
\mathcal{F}_f^{LL} = & 2\sqrt{\frac{2}{3}} \pi M^4 f_B C_f f_D \int_0^1 dx_2 \int_0^\infty b_1 b_2 db_1 db_2 \exp(-\frac{\omega_B^2 b_1^2}{2}) \\
& \{[\psi^L(x_2, b_2) (r_{J/\psi}^2 - 1) (2r_b - x_2) + r_{J/\psi} \psi^t(x_2, b_2) (r_b - 2x_2)] \\
& E_{ab}(t_a) h(\alpha_e, \beta_a, b_1, b_2) S_t(x_2)] \\
& - [\psi^L(x_2, b_2) (r_c + r_\psi^2)] E_{ab}(t_b) h(\alpha_e, \beta_b, b_2, b_1) S_t(x_1)]\}, \tag{A32}
\end{aligned}$$

$$\begin{aligned}
\mathcal{M}_f^{LL} = & \frac{8}{3}\pi M^4 f_B C_f \int_0^1 dx_2 dx_3 \int_0^\infty b_1 b_3 db_1 db_3 \phi_D(x_3, b_3) \exp(-\omega_B^2 \frac{b_1^2}{2}) \times \\
& \{[r_{J/\psi} \psi^t(x_2, b_1) (r_c + x_2 - 1) - \psi^L(x_2, b_1) (x_3 (1 - 2r_\psi^2) - r_c)] \\
& E_{cd}(t_c) h(\beta_c, \alpha_e, b_3, b_1) + [r_{J/\psi} \psi^t(x_2, b_1) (r_c + x_2 - 1) - \\
& \psi^L(x_2, b_1) (2r_c - 2(x_3 - 1)r_\psi^2 + x_2 + x_3 - 2)] \\
& E_{cd}(t_d) h(\beta_d, \alpha_e, b_3, b_1)\}, \tag{A33}
\end{aligned}$$

$$\begin{aligned}
\mathcal{F}_a^{LL} = & -8\pi M^4 f_B C_f \int_0^1 dx_2 dx_3 \int_0^\infty b_2 b_3 db_2 db_3 \phi_D(x_3, b_3) \times \\
& \{[\psi^L(x_2, b_2) ((2x_3 - 1)r_{J/\psi}^2 - x_3 + 1)] E_{ef}(t_e) h(\alpha_a, \beta_e, b_2, b_3) \\
& - [2(x_2 - 1)r_D r_{J/\psi} \psi^t(x_2, b_2) - x_2 \psi^L(x_2, b_2) (r_{J/\psi}^2 - 1)] \\
& E_{ef}(t_f) h(\alpha_a, \beta_f, b_3, b_2)\}, \tag{A34}
\end{aligned}$$

$$\begin{aligned}
\mathcal{M}_a^{LL} = & \frac{8}{3}\pi M^4 f_B C_f \int_0^1 dx_2 dx_3 \int_0^\infty b_1 b_2 db_1 db_2 \phi_D(x_3, b_2) \exp(-\omega_B^2 \frac{b_1^2}{2}) \times \\
& \{[x_2 \psi^L(x_2, b_2) (2r_{J/\psi}^2 - 1) - (x_2 + x_3 - 1)r_D r_{J/\psi} \psi^t(x_2, b_2)] \\
& E_{gh}(t_g) h(\beta_g, \alpha_a, b_1, b_2) - [\psi^L(x_2, b_2) (r_b (r_\psi^2 - 1) - r_c + x_3 (1 - 2r_\psi^2)) \\
& + (x_2 + x_3 - 1)r_D r_{J/\psi} \psi^t(x_2, b_2)] E_{gh}(t_h) h(\beta_h, \alpha_a, b_1, b_2)\}, \tag{A35}
\end{aligned}$$

$$\begin{aligned}
\mathcal{F}_s^{LL} = \mathcal{F}_s^{LR} = & 2\sqrt{\frac{2}{3}}\pi M^4 f_B C_f f_{J/\psi} \int_0^1 dx_2 \int_0^\infty b_1 b_2 db_1 db_2 \phi_D(x_2, b_2) \exp(-\frac{\omega_B^2 b_1^2}{2}) \\
& \{[r_D (r_b - 2x_2) + r_\psi^2 (2r_b - 2x_2 + 1) - 2r_b + x_2] \\
& E_{ab}(t_{as}) h(\alpha_{es}, \beta_{as}, b_1, b_2) S_t(x_2) + \\
& (r_c - 2r_D) E_{ab}(t_{bs}) h(\alpha_{es}, \beta_{bs}, b_2, b_1) S_t(x_1)]\}, \tag{A36}
\end{aligned}$$

$$\begin{aligned}
\mathcal{M}_s^{LL} = & -\frac{8}{3}\pi M^4 f_B C_f \int_0^1 dx_2 dx_3 \int_0^\infty b_1 b_3 db_1 db_3 \phi_D(x_2, b_1) \psi^L(x_3, b_3) \exp(-\omega_B^2 \frac{b_1^2}{2}) \\
& \{[-x_1 + (x_2 - 1)r_D + x_3 (1 - 2r_{J/\psi}^2)] E_{cd}(t_{cs}) h(\beta_{cs}, \alpha_{es}, b_3, b_1) \\
& + [2r_c - (x_2 - 1)r_D - 2(x_2 - 1)r_{J/\psi}^2 + x_2 + x_3 - 2] \\
& E_{cd}(t_{ds}) h(\beta_{ds}, \alpha_{es}, b_3, b_1)\}, \tag{A37}
\end{aligned}$$

$$\begin{aligned}
\mathcal{M}_f^{LR} = & \frac{8}{3}\pi M^4 f_B C_f \int_0^1 dx_2 dx_3 \int_0^\infty b_1 b_3 db_1 db_3 \phi_D(x_3, b_3) \exp(-\omega_B^2 \frac{b_1^2}{2}) \times \\
& \{r_D [x_3 \psi^L(x_2, b_1) - (x_2 + x_3 - 1)r_{J/\psi} \psi^t(x_2, b_1)] E_{cd}(t_c) h(\beta_c, \alpha_e, b_3, b_1) \\
& + [\psi^L(x_2, b_1) ((x_3 - 1)r_D - r_c) + r_{J/\psi} \psi^t(x_2, b_1) (r_c + (x_2 - x_3)r_D)] \\
& E_{cd}(t_d) h(\beta_d, \alpha_e, b_3, b_1)\}, \tag{A38}
\end{aligned}$$

$$\begin{aligned}
\mathcal{M}_a^{LR} = & -\frac{8}{3}\pi M^4 f_B C_f \int_0^1 dx_2 dx_3 \int_0^\infty b_1 b_2 db_1 db_2 \phi_D(x_3, b_2) \exp(-\omega_B^2 \frac{b_1^2}{2}) \times \\
& \{[(x_3 - 1) r_D \psi^L(x_2, b_2) - r_{J/\psi} \psi^t(x_2, b_2) (2r_c - x_2)] E_{gh}(t_g) h(\beta_g, \alpha_a, b_1, b_2) \\
& - [r_D \psi^L(x_2, b_2) (r_b + x_3) - r_{J/\psi} \psi^t(x_2, b_2) (r_b - r_c - x_2 + 1)] \\
& E_{gh}(t_h) h(\beta_h, \alpha_a, b_1, b_2)\}, \tag{A39}
\end{aligned}$$

$$\begin{aligned}
\mathcal{M}_s^{SP} = & \frac{8}{3}\pi M^4 f_B C_f \int_0^1 dx_2 dx_3 \int_0^\infty b_1 b_3 db_1 db_3 \phi_D(x_2, b_1) \exp(-\omega_B^2 \frac{b_1^2}{2}) \\
& \{[2r_c - (x_2 - 1) (r_D + 2r_\psi^2 - 1) - x_3] \psi^L(x_3, b_3) \\
& E_{cd}(t_{cs}) h(\beta_{cs}, \alpha_{es}, b_3, b_1) + [r_c r_{J/\psi} \psi^t(x_3, b_3) + \psi^L(x_3, b_3) \\
& (-r_c + (x_2 - 1) r_D + (x_3 - 1) (2r_\psi^2 - 1))] \\
& E_{cd}(t_{ds}) h(\beta_{ds}, \alpha_{es}, b_3, b_1)\}, \tag{A40}
\end{aligned}$$

$$\begin{aligned}
\mathcal{F}_a^{SP} = & 16\pi M^4 f_B C_f \int_0^1 dx_2 dx_3 \int_0^\infty b_2 b_3 db_2 db_3 \phi_D(x_3, b_3) \times \\
& \{\psi^L(x_2, b_2) (r_c - (x_3 - 1) r_D) E_{ef}(t_e) h(\alpha_a, \beta_e, b_2, b_3) \\
& + [2r_D \psi^L(x_2, b_2) - x_2 r_{J/\psi} \psi^t(x_2, b_2)] E_{ef}(t_f) h(\alpha_a, \beta_f, b_3, b_2)\}, \tag{A41}
\end{aligned}$$

$$\begin{aligned}
\mathcal{F}_f^{SP} = & -4\sqrt{\frac{2}{3}}\pi M^4 f_B C_f f_D r_D \int_0^1 dx_2 \int_0^\infty b_1 b_2 db_1 db_2 \exp(-\frac{\omega_B^2 b_1^2}{2}) \\
& [(r_b - 2) \psi^L(x_2, b_2) - (x_2 - 1) r_{J/\psi} \psi^t(x_2, b_2)] \\
& E_{ab}(t_a) h(\alpha_e, \beta_a, b_1, b_2) S_t(x_2), \tag{A42}
\end{aligned}$$

where the expressions of  $\beta_{a,b,c,d}$  and  $\alpha_e$  are the similar to those of Eq. (A21), but with the replacement  $r_{\eta_c} \rightarrow r_{J/\psi}$ .

## 6. Factorization formulas for $B_c \rightarrow J/\Psi D_{(s)}^*$

$$\begin{aligned}
\mathcal{F}_f^{LL,L} = & 2\sqrt{\frac{2}{3(1-r_{J/\psi}^2)}}\pi M^4 f_B C_f f_D \int_0^1 dx_2 \int_0^\infty b_1 b_2 db_1 db_2 \exp(-\frac{\omega_B^2 b_1^2}{2}) \\
& \{[\psi^L(x_2, b_2) (r_{J/\psi}^2 - 1) (2r_b - x_2) + r_{J/\psi} \psi^t(x_2, b_2) (r_b - 2x_2)] \\
& E_{ab}(t_a) h(\alpha_e, \beta_a, b_1, b_2) S_t(x_2)] \\
& - [\psi^L(x_2, b_2) (r_c + r_\psi^2)] E_{ab}(t_b) h(\alpha_e, \beta_b, b_2, b_1) S_t(x_1)]\}, \tag{A43}
\end{aligned}$$

$$\begin{aligned}
\mathcal{M}_f^{LL,L} &= \frac{8\pi M^4 f_B C_f}{3\sqrt{1-r_{J/\psi}^2}} \int_0^1 dx_2 dx_3 \int_0^\infty b_1 b_3 db_1 db_3 \phi_D(x_3, b_3) \exp(-\omega_B^2 \frac{b_1^2}{2}) \times \\
&\quad \{[r_{J/\psi} \psi^t(x_2, b_1) (r_c + x_2 - 1) - \psi^L(x_2, b_1) (r_c + x_3 (2r_{J/\psi}^2 - 1))] \\
&\quad E_{cd}(t_c) h(\beta_c, \alpha_e, b_3, b_1) - [\psi^L(x_2, b_1) (2r_c - 2(x_3 - 1)r_{J/\psi}^2 + x_2 + x_3 - 2) \\
&\quad - r_{J/\psi} \psi^t(x_2, b_1) (r_c + x_2 - 1)] E_{cd}(t_d) h(\beta_d, \alpha_e, b_3, b_1)\}, \tag{A44}
\end{aligned}$$

$$\begin{aligned}
\mathcal{F}_a^{LL,L} &= -\frac{8\pi M^4 f_B C_f}{\sqrt{1-r_{J/\psi}^2}} \int_0^1 dx_2 dx_3 \int_0^\infty b_2 b_3 db_2 db_3 \phi_D(x_3, b_3) \psi^L(x_2, b_2) \\
&\quad \{[(2x_3 - 1)r_{J/\psi}^2 - x_3 + 1] E_{ef}(t_e) h(\alpha_a, \beta_e, b_2, b_3) \\
&\quad - x_2 (1 - r_{J/\psi}^2) E_{ef}(t_f) h(\alpha_a, \beta_f, b_3, b_2)\}, \tag{A45}
\end{aligned}$$

$$\begin{aligned}
\mathcal{M}_a^{LL,L} &= \frac{8\pi M^4 f_B C_f}{3\sqrt{1-r_{J/\psi}^2}} \int_0^1 dx_2 dx_3 \int_0^\infty b_1 b_2 db_1 db_2 \phi_D(x_3, b_2) \exp(-\omega_B^2 \frac{b_1^2}{2}) \times \\
&\quad \{[x_2 \psi^L(x_2, b_2) (2r_{J/\psi}^2 - 1) - (x_2 - x_3 + 1) r_D r_{J/\psi} \psi^t(x_2, b_2)] \\
&\quad E_{gh}(t_g) h(\beta_g, \alpha_a, b_1, b_2) + [(x_2 - x_3 - 1) r_D r_{J/\psi} \psi^t(x_2, b_2) - \psi^L(x_2, b_2) \\
&\quad (r_b (r_{J/\psi}^2 - 1) - r_c - x_3 (2r_{J/\psi}^2 - 1))] E_{gh}(t_h) h(\beta_h, \alpha_a, b_1, b_2)\}, \tag{A46}
\end{aligned}$$

$$\begin{aligned}
\mathcal{F}_s^{LL,L} &= \mathcal{F}_s^{LR,L} = 2\sqrt{\frac{2}{3(1-r_{J/\psi}^2)}} \pi M^4 f_B C_f f_{J/\psi} \int_0^1 dx_2 \int_0^\infty b_1 b_2 db_1 db_2 \phi_D(x_2, b_2) \\
&\quad \exp(-\frac{\omega_B^2 b_1^2}{2}) \{[r_D (r_b - 2x_2) + r_{J/\psi}^2 (2r_b - 2x_2 + 1) - 2r_b + x_2] \\
&\quad E_{ab}(t_{as}) h(\alpha_{es}, \beta_{as}, b_1, b_2) S_t(x_2) - r_c E_{ab}(t_{bs}) h(\alpha_{es}, \beta_{bs}, b_2, b_1) S_t(x_1)\} \tag{A47}
\end{aligned}$$

$$\begin{aligned}
\mathcal{M}_s^{LL,L} &= \frac{8\pi M^4 f_B C_f}{3\sqrt{1-r_{J/\psi}^2}} \int_0^1 dx_2 dx_3 \int_0^\infty b_1 b_3 db_1 db_3 \phi_D(x_2, b_1) \psi^L(x_3, b_3) \exp(-\omega_B^2 \frac{b_1^2}{2}) \\
&\quad \{[x_1 + (x_2 - 1) r_D + x_3 (2r_{J/\psi}^2 - 1)] E_{cd}(t_{cs}) h(\beta_{cs}, \alpha_{es}, b_3, b_1) \\
&\quad - [2r_c - (x_2 - 1) r_D - 2(x_2 - 1) r_{J/\psi}^2 + x_2 + x_3 - 2] \\
&\quad E_{cd}(t_{ds}) h(\beta_{ds}, \alpha_{es}, b_3, b_1)\}, \tag{A48}
\end{aligned}$$

$$\begin{aligned}
\mathcal{M}_f^{LR,L} &= \frac{8\pi M^4 f_B C_f}{3\sqrt{1-r_{J/\psi}^2}} \int_0^1 dx_2 dx_3 \int_0^\infty b_1 b_3 db_1 db_3 \phi_D(x_3, b_3) \exp(-\omega_B^2 \frac{b_1^2}{2}) \times \\
&\quad \{[r_D (x_3 \psi^L(x_2, b_1) + (x_2 - x_3 - 1) r_{J/\psi} \psi^t(x_2, b_1))] E_{cd}(t_c) h(\beta_c, \alpha_e, b_3, b_1) \\
&\quad + [r_{J/\psi} \psi^t(x_2, b_1) (r_c + (x_2 + x_3 - 2) r_D) - \psi^L(x_2, b_1) (r_c + (x_3 - 1) r_D)] \\
&\quad E_{cd}(t_d) h(\beta_d, \alpha_e, b_3, b_1)\}, \tag{A49}
\end{aligned}$$

$$\begin{aligned}
\mathcal{M}_a^{LR,L} = & -\frac{8\pi M^4 f_B C_f}{3\sqrt{1-r_{J/\psi}^2}} \int_0^1 dx_2 dx_3 \int_0^\infty b_1 b_2 db_1 db_2 \phi_D(x_3, b_2) \exp(-\omega_B^2 \frac{b_1^2}{2}) \times \\
& \{[(x_3 - 1) r_D \psi^L(x_2, b_2) - r_{J/\psi} \psi^t(x_2, b_2) (2r_c - x_2)] E_{gh}(t_g) h(\beta_g, \alpha_a, b_1, b_2) \\
& - [r_{J/\psi} \psi^t(x_2, b_2) (-r_b + r_c + x_2 - 1) + r_D \psi^L(x_2, b_2) (r_b + x_3)] \\
& E_{gh}(t_h) h(\beta_h, \alpha_a, b_1, b_2)\}, \tag{A50}
\end{aligned}$$

$$\begin{aligned}
\mathcal{M}_s^{SP,L} = & \frac{8\pi M^4 f_B C_f}{3\sqrt{1-r_{J/\psi}^2}} \int_0^1 dx_2 dx_3 \int_0^\infty b_1 b_3 db_1 db_3 \phi_D(x_2, b_1) \exp(-\omega_B^2 \frac{b_1^2}{2}) \times \\
& \{[\psi^L(x_3, b_3) (2r_c - (x_2 - 1) (r_D + 2r_{J/\psi}^2 - 1) - x_3)] \\
& E_{cd}(t_{cs}) h(\beta_{cs}, \alpha_{es}, b_3, b_1) + [r_c r_{J/\psi} \psi^t(x_3, b_3) + \psi^L(x_3, b_3) \\
& ((x_3 - 1) (2r_{J/\psi}^2 - 1) - (x_2 - 1) r_D - r_c (1 - r_{J/\psi}))] \\
& E_{cd}(t_{ds}) h(\beta_{ds}, \alpha_{es}, b_3, b_1)\}, \tag{A51}
\end{aligned}$$

$$\begin{aligned}
\mathcal{F}_a^{SP,L} = & \frac{16\pi M^4 f_B C_f}{\sqrt{1-r_{J/\psi}^2}} \int_0^1 dx_2 dx_3 \int_0^\infty b_2 b_3 db_2 db_3 \phi_D(x_3, b_3) \times \\
& \{[\psi^L(x_2, b_2) (r_c + (x_3 - 1) r_D)] E_{ef}(t_e) h(\alpha_a, \beta_e, b_2, b_3) - \\
& [x_2 r_{J/\psi} \psi^t(x_2, b_2)] E_{ef}(t_f) h(\alpha_a, \beta_f, b_3, b_2)\}, \tag{A52}
\end{aligned}$$

$$\begin{aligned}
\mathcal{F}_f^{LL,N} = & 2\sqrt{\frac{2}{3}} \pi M^4 f_B C_f f_D r_D \int_0^1 dx_2 \int_0^\infty b_1 b_2 db_1 db_2 \exp(-\frac{\omega_B^2 b_1^2}{2}) \\
& \{[(r_\psi \psi^T (-4r_b + x_2 + 1) + (r_b - 2) \psi^V)] \\
& E_{ab}(t_a) h(\alpha_e, \beta_a, b_1, b_2) S_t(x_2) \\
& - [r_\psi \psi^T] E_{ab}(t_b) h(\alpha_e, \beta_b, b_2, b_1) S_t(x_1)]\}, \tag{A53}
\end{aligned}$$

$$\begin{aligned}
\mathcal{F}_f^{LL,T} = & 2\sqrt{\frac{2}{3}} \pi M^4 f_B C_f f_D r_D \int_0^1 dx_2 \int_0^\infty b_1 b_2 db_1 db_2 \exp(-\frac{\omega_B^2 b_1^2}{2}) \\
& \{[(r_b - 2) \psi^V - (x_2 - 1) r_\psi \psi^T] \\
& E_{ab}(t_a) h(\alpha_e, \beta_a, b_1, b_2) S_t(x_2) \\
& - [r_\psi \psi^T] E_{ab}(t_b) h(\alpha_e, \beta_b, b_2, b_1) S_t(x_1)]\}, \tag{A54}
\end{aligned}$$

$$\begin{aligned}
\mathcal{M}_f^{LL,N} = & \frac{8}{3} \pi M^4 f_B C_f r_D \int_0^1 dx_2 dx_3 \int_0^\infty b_1 b_3 db_1 db_3 \phi_D(x_3, b_3) \exp(-\omega_B^2 \frac{b_1^2}{2}) \times \\
& \{[(x_3 \psi^V(x_2, b_1)] E_{cd}(t_c) h(\beta_c, \alpha_e, b_3, b_1) \\
& + [(2(x_2 + x_3 - 2) r_\psi \psi^T - (x_3 - 1) \psi^V)] E_{cd}(t_d) h(\beta_d, \alpha_e, b_3, b_1)\}. \tag{A55}
\end{aligned}$$

$$\begin{aligned}
\mathcal{M}_f^{LL,T} &= \frac{8}{3}\pi M^4 f_B C_f r_D \int_0^1 dx_2 dx_3 \int_0^\infty b_1 b_3 db_1 db_3 \phi_D(x_3, b_3) \exp(-\omega_B^2 \frac{b_1^2}{2}) \times \\
&\quad \{(x_3 \psi^V(x_2, b_1)) E_{cd}(t_c) h(\beta_c, \alpha_e, b_3, b_1) \\
&\quad + [\psi^V(x_2, b_1)(1-x_3)] E_{cd}(t_d) h(\beta_d, \alpha_e, b_3, b_1)\}. \tag{A56}
\end{aligned}$$

$$\begin{aligned}
\mathcal{F}_a^{LL,N} &= -8\pi M^4 f_B C_f r_\psi \int_0^1 dx_2 dx_3 \int_0^\infty b_2 b_3 db_2 db_3 \phi_D(x_3, b_3) \psi^T(x_2, b_2) \\
&\quad \{[(r_c + (x_3 - 2)r_D)] E_{ef}(t_e) h(\alpha_a, \beta_e, b_2, b_3) \\
&\quad + (x_2 + 1)r_D E_{ef}(t_f) h(\alpha_a, \beta_f, b_3, b_2)\}. \tag{A57}
\end{aligned}$$

$$\begin{aligned}
\mathcal{F}_a^{LL,T} &= -8\pi M^4 f_B C_f r_\psi \int_0^1 dx_2 dx_3 \int_0^\infty b_2 b_3 db_2 db_3 \phi_D(x_3, b_3) \psi^T(x_2, b_2) \\
&\quad \{[(r_c + x_3 r_D)] E_{ef}(t_e) h(\alpha_a, \beta_e, b_2, b_3) \\
&\quad - (x_2 - 1)r_D E_{ef}(t_f) h(\alpha_a, \beta_f, b_3, b_2)\}. \tag{A58}
\end{aligned}$$

$$\begin{aligned}
\mathcal{M}_a^{LL,N} &= \frac{8}{3}\pi M^4 f_B C_f r_{J/\psi} \int_0^1 dx_2 dx_3 \int_0^\infty b_1 b_2 db_1 db_2 \phi_D(x_3, b_2) \exp(-\omega_B^2 \frac{b_1^2}{2}) \\
&\quad \{[x_2 r_{J/\psi} \psi^V(x_2, b_2)] E_{gh}(t_g) h(\beta_g, \alpha_a, b_1, b_2) - [2r_b r_D \psi^T(x_2, b_2) \\
&\quad + (x_2 - 1)r_{J/\psi} \psi^V(x_2, b_2)] E_{gh}(t_h) h(\beta_h, \alpha_a, b_1, b_2)\}. \tag{A59}
\end{aligned}$$

$$\begin{aligned}
\mathcal{M}_a^{LL,T} &= \frac{8}{3}\pi M^4 f_B C_f r_{J/\psi}^2 \int_0^1 dx_2 dx_3 \int_0^\infty b_1 b_2 db_1 db_2 \phi_D(x_3, b_2) \psi^V(x_2, b_2) \exp(-\frac{\omega_B^2 b_1^2}{2}) \\
&\quad \{x_2 E_{gh}(t_g) h(\beta_g, \alpha_a, b_1, b_2) - (x_2 - 1) E_{gh}(t_h) h(\beta_h, \alpha_a, b_1, b_2)\}. \tag{A60}
\end{aligned}$$

$$\begin{aligned}
\mathcal{F}_s^{LL,N} &= -2\sqrt{\frac{2}{3}}\pi M^4 f_B C_f f_{J/\psi} r_{J/\psi} \int_0^1 dx_2 \int_0^\infty b_1 b_2 db_1 db_2 \phi_D(x_2, b_2) \exp(-\frac{\omega_B^2 b_1^2}{2}) \\
&\quad \{[(r_b(4r_D - 1) - (x_2 + 1)r_D + 2)] E_{ab}(t_{as}) h(\alpha_{es}, \beta_{as}, b_1, b_2) S_t(x_2) \\
&\quad + r_D E_{ab}(t_{bs}) h(\alpha_{es}, \beta_{bs}, b_2, b_1) S_t(x_1)]\}, \tag{A61}
\end{aligned}$$

$$\begin{aligned}
\mathcal{F}_s^{LL,T} &= -2\sqrt{\frac{2}{3}}\pi M^4 f_B C_f f_{J/\psi} r_{J/\psi} \int_0^1 dx_2 \int_0^\infty b_1 b_2 db_1 db_2 \phi_D(x_2, b_2) \exp(-\frac{\omega_B^2 b_1^2}{2}) \\
&\quad \{[(r_b - (x_2 - 1)r_D - 2)] E_{ab}(t_{as}) h(\alpha_{es}, \beta_{as}, b_1, b_2) S_t(x_2) \\
&\quad - r_D E_{ab}(t_{bs}) h(\alpha_{es}, \beta_{bs}, b_2, b_1) S_t(x_1)]\}, \tag{A62}
\end{aligned}$$

$$\begin{aligned}
\mathcal{M}_s^{LL,N} &= \frac{8}{3}\pi M^4 f_B C_f r_{J/\psi} \int_0^1 dx_2 dx_3 \int_0^\infty b_1 b_3 db_1 db_3 \phi_D(x_2, b_1) \psi^T(x_3, b_3) \\
&\quad \exp(-\omega_B^2 \frac{b_1^2}{2}) \{(x_3 - x_1) E_{cd}(t_{cs}) h(\beta_{cs}, \alpha_{es}, b_3, b_1) \\
&\quad + (2(x_2 + x_3 - 2)r_D - x_3 - x_1 + 1) E_{cd}(t_{ds}) h(\beta_{ds}, \alpha_{es}, b_3, b_1)\} \tag{A63}
\end{aligned}$$



$$\begin{aligned}
\mathcal{M}_s^{LL,T} &= -\frac{8}{3}\pi M^4 x_3 f_B C_f r_{J/\psi} \int_0^1 dx_2 dx_3 \int_0^\infty b_1 b_3 db_1 db_3 \phi_D(x_2, b_1) \psi^T(x_3, b_3) \\
&\quad \exp(-\omega_B^2 \frac{b_1^2}{2}) \{ (x_3 - x_1) E_{cd}(t_{cs}) h(\beta_{cs}, \alpha_{es}, b_3, b_1) \\
&\quad - (x_1 + x_3 - 1) E_{cd}(t_{ds}) h(\beta_{ds}, \alpha_{es}, b_3, b_1) \}, \tag{A64}
\end{aligned}$$

$$\begin{aligned}
\mathcal{F}_s^{LR,N} &= -2\sqrt{\frac{2}{3}}\pi M^4 f_B C_f f_{J/\psi} r_{J/\psi} \int_0^1 dx_2 \int_0^\infty b_1 b_2 db_1 db_2 \phi_D(x_2, b_2) \exp(-\frac{\omega_B^2 b_1^2}{2}) \\
&\quad \{ [(r_b (4r_D - 1) - (x_2 + 1) r_D + 2) E_{ab}(t_{as}) h(\alpha_{es}, \beta_{as}, b_1, b_2) S_t(x_2)] \\
&\quad - r_D E_{ab}(t_{bs}) h(\alpha_{es}, \beta_{bs}, b_2, b_1) S_t(x_1)] \}, \tag{A65}
\end{aligned}$$

$$\begin{aligned}
\mathcal{F}_s^{LR,T} &= -2\sqrt{\frac{2}{3}}\pi M^4 f_B C_f f_{J/\psi} r_{J/\psi} \int_0^1 dx_2 \int_0^\infty b_1 b_2 db_1 db_2 \phi_D(x_2, b_2) \exp(-\frac{\omega_B^2 b_1^2}{2}) \\
&\quad \{ [(r_b - (x_2 - 1) r_D - 2) E_{ab}(t_{as}) h(\alpha_{es}, \beta_{as}, b_1, b_2) S_t(x_2)] \\
&\quad + r_D E_{ab}(t_{bs}) h(\alpha_{es}, \beta_{bs}, b_2, b_1) S_t(x_1)] \}, \tag{A66}
\end{aligned}$$

$$\begin{aligned}
\mathcal{M}_f^{LR,N} &= \mathcal{M}_f^{LR,T} = \frac{8}{3}\pi M^4 f_B C_f r_{J/\psi} \int_0^1 dx_2 dx_3 \int_0^\infty b_1 b_3 db_1 db_3 \phi_D(x_3, b_3) \exp(-\omega_B^2 \frac{b_1^2}{2}) \\
&\quad \{ [(\psi^T(x_2, b_1) (r_c + x_2 - 1) - (x_2 - 1) r_{J/\psi} \psi^V(x_2, b_1))] \\
&\quad (E_{cd}(t_c) h(\beta_c, \alpha_e, b_3, b_1) + E_{cd}(t_d) h(\beta_d, \alpha_e, b_3, b_1)) \}. \tag{A67}
\end{aligned}$$

$$\begin{aligned}
\mathcal{M}_a^{LR,N} &= \mathcal{M}_a^{LR,T} = -\frac{8}{3}\pi M^4 f_B C_f \int_0^1 dx_2 dx_3 \int_0^\infty b_1 b_2 db_1 db_2 \phi_D(x_3, b_2) \exp(-\omega_B^2 \frac{b_1^2}{2}) \\
&\quad \{ [(x_3 - 1) r_D \psi^V(x_2, b_2) - r_{J/\psi} \psi^T(x_2, b_2) (2r_c - x_2)] E_{gh}(t_g) h(\beta_g, \alpha_a, b_1, b_2) \\
&\quad - [r_{J/\psi} \psi^T(x_2, b_2) (-r_b + r_c + x_2 - 1) + r_D \psi^V(x_2, b_2) (r_b + x_3)] \\
&\quad E_{gh}(t_h) h(\beta_h, \alpha_a, b_1, b_2) \}. \tag{A68}
\end{aligned}$$

$$\begin{aligned}
\mathcal{M}_s^{SP,N} &= \frac{4}{3}\pi M^4 f_B C_f r_{J/\psi} \int_0^1 dx_2 dx_3 \int_0^\infty b_1 b_3 db_1 db_3 \phi_D(x_2, b_1) \psi^T(x_3, b_3) \exp(-\omega_B^2 \frac{b_1^2}{2}) \\
&\quad \{ [(2(x_2 - x_3 - 1) r_D + x_3 - x_1)] \\
&\quad E_{cd}(t_{cs}) h(\beta_{cs}, \alpha_{es}, b_3, b_1) - (x_1 + x_3 - 1) E_{cd}(t_{ds}) h(\beta_{ds}, \alpha_{es}, b_3, b_1) \}. \tag{A69}
\end{aligned}$$

$$\begin{aligned}
\mathcal{M}_s^{SP,T} &= -\frac{4}{3}\pi M^4 f_B C_f r_{J/\psi} \int_0^1 dx_2 dx_3 \int_0^\infty b_1 b_3 db_1 db_3 \phi_D(x_2, b_1) \psi^T(x_3, b_3) \exp(-\omega_B^2 \frac{b_1^2}{2}) \\
&\quad \{ (x_3 - x_1) E_{cd}(t_{cs}) h(\beta_{cs}, \alpha_{es}, b_3, b_1) - (x_1 + x_3 - 1) E_{cd}(t_{ds}) h(\beta_{ds}, \alpha_{es}, b_3, b_1) \}. \tag{A70}
\end{aligned}$$

$$\begin{aligned}
\mathcal{F}_a^{SP,N} = \mathcal{F}_a^{SP,T} &= 16\pi M^4 f_B C_f \int_0^1 dx_2 dx_3 \int_0^\infty b_2 b_3 db_2 db_3 \phi_D(x_3, b_3) \\
&\quad \{r_{J/\psi} \psi^T(x_2, b_2) E_{ef}(t_e) h(\alpha_a, \beta_e, b_2, b_3) + r_D \psi^V(x_2, b_2) E_{ef}(t_f) h(\alpha_a, \beta_f, b_3, b_2)\},
\end{aligned} \tag{A71}$$

where the expressions of  $\beta_{a,b,c,d}$  and  $\alpha_e$  are the similar to those of Eq. (A21), but with the replacement  $r_{\eta_c} \rightarrow r_{J/\psi}$ .

## Appendix B: scales and related functions in hard kernel

We show here the functions  $h$ , coming from the Fourier transform of virtual quark and gluon propagators:

$$\begin{aligned}
h(\alpha, \beta, b_1, b_2) &= h_1(\alpha, b_1) \times h_2(\beta, b_1, b_2), \\
h_1(\alpha, b_1) &= \begin{cases} K_0(\sqrt{\alpha} b_1) & \alpha > 0 \\ K_0(i\sqrt{-\alpha} b_1) & \alpha < 0 \end{cases} \\
h_2(\beta, b_1, b_2) &= \begin{cases} \theta(b_1 - b_2) I_0(\sqrt{\beta} b_2) K_0(\sqrt{\beta} b_1) + (b_1 \leftrightarrow b_2) & \beta > 0 \\ \theta(b_1 - b_2) J_0(\sqrt{-\beta} b_2) K_0(i\sqrt{-\beta} b_1) + (b_1 \leftrightarrow b_2) & \beta < 0 \end{cases} \tag{B1}
\end{aligned}$$

where  $J_0$  is the Bessel function and  $K_0, I_0$  are modified Bessel function with  $K_0(ix) = \frac{\pi}{2}(-N_0(x) + iJ_0(x))$ . The hard scale  $t$  is chosen as the maximum of the virtuality of the internal momentum transition in the hard amplitudes, including  $1/b_i (i = 1, 2, 3)$ :

$$\begin{aligned}
t_{a(as)} &= \max(\sqrt{|\alpha_{e(es)}|}, \sqrt{|\beta_{a(as)}|}, 1/b_1, 1/b_2), & t_{b(bs)} &= \max(\sqrt{|\alpha_{e(es)}|}, \sqrt{|\beta_{b(bs)}|}, 1/b_1, 1/b_2), \\
t_{c(cs)} &= \max(\sqrt{|\alpha_{e(es)}|}, \sqrt{|\beta_{c(cs)}|}, 1/b_1, 1/b_3), & t_{d(ds)} &= \max(\sqrt{|\alpha_{e(es)}|}, \sqrt{|\beta_{d(ds)}|}, 1/b_1, 1/b_3), \\
t_e &= \max(\sqrt{|\alpha_a|}, \sqrt{|\beta_e|}, 1/b_2, 1/b_3), & t_f &= \max(\sqrt{|\alpha_a|}, \sqrt{|\beta_f|}, 1/b_2, 1/b_3), \\
t_g &= \max(\sqrt{|\alpha_a|}, \sqrt{|\beta_g|}, 1/b_1, 1/b_2), & t_h &= \max(\sqrt{|\alpha_a|}, \sqrt{|\beta_h|}, 1/b_1, 1/b_2).
\end{aligned} \tag{B2}$$

The function  $E_{ij}(t)$  is defined by

$$E_{ab,cd,ef,gh}(t) = \alpha_s(t) S_{ab,cd,ef,gh}(t), \tag{B3}$$

where the Sudakov factors can be written as

$$\begin{aligned}
S_{ab}(t) &= s\left(\frac{M_B}{\sqrt{2}}x_1, b_1\right) + s\left(\frac{M_B}{\sqrt{2}}x_2, b_2\right) + s\left(\frac{M_B}{\sqrt{2}}(1-x_2), b_2\right) \\
&\quad + \frac{5}{3} \int_{1/b_1}^t \frac{d\mu}{\mu} \gamma_q(\mu) + 2 \int_{1/b_2}^t \frac{d\mu}{\mu} \gamma_q(\mu), \\
S_{cd}(t) &= s\left(\frac{M_B}{\sqrt{2}}x_1, b_1\right) + s\left(\frac{M_B}{\sqrt{2}}x_2, b_1\right) + s\left(\frac{M_B}{\sqrt{2}}(1-x_2), b_1\right) \\
&\quad + s\left(\frac{M_B}{\sqrt{2}}x_3, b_3\right) + s\left(\frac{M_B}{\sqrt{2}}(1-x_3), b_3\right) \\
&\quad + \frac{11}{3} \int_{1/b_1}^t \frac{d\mu}{\mu} \gamma_q(\mu) + 2 \int_{1/b_3}^t \frac{d\mu}{\mu} \gamma_q(\mu), \\
S_{ef}(t) &= s\left(\frac{M_B}{\sqrt{2}}x_2, b_2\right) + s\left(\frac{M_B}{\sqrt{2}}(1-x_2), b_2\right) + s\left(\frac{M_B}{\sqrt{2}}x_3, b_3\right) \\
&\quad + s\left(\frac{M_B}{\sqrt{2}}(1-x_3), b_3\right) + 2 \int_{1/b_2}^t \frac{d\mu}{\mu} \gamma_q(\mu) + 2 \int_{1/b_3}^t \frac{d\mu}{\mu} \gamma_q(\mu), \\
S_{gh}(t) &= s\left(\frac{M_B}{\sqrt{2}}x_1, b_1\right) + s\left(\frac{M_B}{\sqrt{2}}x_2, b_2\right) + s\left(\frac{M_B}{\sqrt{2}}(1-x_2), b_2\right) + s\left(\frac{M_B}{\sqrt{2}}x_3, b_2\right) \\
&\quad + s\left(\frac{M_B}{\sqrt{2}}(1-x_3), b_2\right) + \frac{5}{3} \int_{1/b_1}^t \frac{d\mu}{\mu} \gamma_q(\mu) + 4 \int_{1/b_2}^t \frac{d\mu}{\mu} \gamma_q(\mu), \tag{B4}
\end{aligned}$$

where the functions  $s(Q, b)$  are defined in Appendix A of [25].  $\gamma_q = -\alpha_s/\pi$  is the anomalous dimension of the quark.

- 
- [1] F. Abe, et al. [CDF Collaboration], Phys. Rev. Lett. **81**, 2432 (1998).
  - [2] A. Abulencia et al. [CDF Collaboration], Phys. Rev. Lett. **97**, 012002(2006).
  - [3] V. M. Abazov et al. [D0 Collaboration], Phys. Rev. Lett. **102**, 092001(2009).
  - [4] T. Aaltonen et al. [CDF Collaboration], Phys. Rev. Lett. **100**, 182002(2008).
  - [5] V. M. Abazov et al. [D0 Collaboration], Phys. Rev. Lett. **101**, 012001(2008).
  - [6] N. Brambilla et al.(Quarkonium Working Group), Report No. CERN-2005-005;M. P. Altarelli and F. Teubert,Int. J. Mod. Phys. A **23**, 5117 (2008).
  - [7] R. Aaij et al. [LHCb Collaboration], Phys. Rev. Lett. **109**, 232001(2012).
  - [8] R. Aaij et al. [LHCb Collaboration], Phys. Rev. Lett. **108**, 251802(2012).
  - [9] R. Aaij et al. [LHCb Collaboration], J. High Energy Phys. **09** (2013) 075.
  - [10] R. Aaij et al. [LHCb Collaboration], Phys. Rev. D **87**, 071103 (2013).

- [11] R. Aaij et al. [LHCb Collaboration], Phys. Rev. D **87**, 112012 (2013).
- [12] R. Aaij et al. [LHCb Collaboration], J. High Energy Phys. **11** (2013) 094.
- [13] R. Aaij et al. [LHCb Collaboration], Phys. Rev. Lett. **111**, 181801 (2013).
- [14] R. Aaij et al. [LHCb Collaboration], J. High Energy Phys. **05** (2014) 148.
- [15] T. Aaltonen et al. [CDF Collaboration], Phys. Rev. D. **87**, 011101(2013).
- [16] N. Brambilla et al., (Quarkonium Working Group), hep-ph/0412158.
- [17] H.-n. Li, and H.L.Yu, Phys. Rev. Lett. **74**, 4388 (1995); H.-n. Li, Phys. Lett. B **348**, 597 (1995).
- [18] X. Liu, Z.-J. Xiao and Cai-Dian Lü, Phys Rev D **81**, 014022 (2010).
- [19] X. Liu and Z.-J. Xiao, Phys Rev D **81**, 074017 (2010).
- [20] Y.Yang, J.Sun and N. Wang, Phys Rev D **81**, 074012 (2010).
- [21] X. Liu and Z.-J. Xiao, Phys Rev D **82**, 054029 (2010).
- [22] X. Liu and Z.-J. Xiao, J Phys G **38**, 035009 (2011).
- [23] Z.-J. Xiao and X. Liu, Phys Rev D **84**, 074033 (2011).
- [24] Z.-J. Xiao and X. Liu, Chin. Sci. Bull. **59**, 3748 (2014).
- [25] J. F. Cheng, D. S. Du, and Cai-Dian Lü, Eur Phys J C **45**, 711 (2006).
- [26] Zhang J and Yu X Q, Eur Phys J C **63**, 435 (2009).
- [27] Z. Rui, Z.-T. Zou, and Cai-Dian Lü, Phys Rev D **86**, 074008 (2012).
- [28] R.Zhou, Z. Zou, and Cai-Dian Lü, Phys Rev D **86**, 074019 (2012).
- [29] Z.-T. Zou, X. Yu and Cai-Dian Lü, Phys Rev D **87**, 074027 (2013).
- [30] J. Sun, D. Du, and Y. Yang, Eur. Phys. J. C **60**, 107 (2009).
- [31] X. Q. Yu and X. L. Zhou, Phys Rev D **81**, 037501 (2010).
- [32] Particle Data Group, Phys Rev D **86**, 010001 (2012).
- [33] H.-N. Li and Hoi-Lai Yu, Phys Rev D **53**, 2480 (1996).
- [34] Cong-Feng Qiao, Peng Sun, Deshan Yang and Rui-Lin Zhu, Phys Rev D **89**, 034008 (2014).
- [35] D. Ebert, R. N. Faustov and V. O. Galkin, Phys Rev D **68**, 094020 (2003).
- [36] Bell G and Feldmann Th, J High Energy Phys **04**, 061(2008); arXiv:hep-ph/0509347 (2005).
- [37] Yu Jia, Jian-Xiong Wang and Deshan Yang, J. High Energy Phys. **10** (2011) 105.

- [38] Wang W, Shen Y L and Cai-Dian Lü, Eur Phys J C **51**, 841 (2007).
- [39] C.W.Bauer, D. Pirjol and I. W. Stewart, Phys. Rev. Lett. **87**, 201806 (2001).
- [40] Ying Li, Cai-Dian Lü and Cong-Feng Qiao, Phys.Rev.D **73**, 094006 (2006).
- [41] C.-H. Chang and H.-N. Li, Phys. Rev. D **55**, 5577 (1997).
- [42] J. C. Collins and D. E. Soper, Nucl. Phys. B **193**, 381 (1981); J. Botts and G. Sterman, Nucl. Phys. B **325**, 62 (1989).
- [43] Cai-Dian Lü and M.-Z. Yang, Eur. Phys. J. C **28**, 515 (2003).
- [44] T. Kurimoto ,H.-N. Li and A. I. Sanda, Phys. Rev. D **67**, 054028 (2003).
- [45] A. V. Manohar and M. B. Wise, Cambridge Monogr. Part. Phys., Nucl. Phys. Cosmol.**10**, 1 (2000).
- [46] Run-Hui Li, Cai-Dian Lü, and Hao Zou, Phys. Rev. D **78**, 014018 (2008); Hao Zou, Run-Hui Li, Xiao-Xia Wang, and Cai-Dian Lü, J. Phys. G **37**, 015002 (2010).
- [47] Run-Hui Li, Cai-Dian Lü, A.I. Sanda and Xiao-Xia Wang Phys. Rev. D **81**, 034006 (2010).
- [48] C.-H. Chang and H.-N. Li, Phys. Rev. D **71**, 114008 (2005).
- [49] V. M. Braun and I. E. Filyanov,Z. Phys. C **48**, 239 (1990); P. Ball, V. M. Braun, Y. Koike, and K. Tanaka,Nucl. Phys. B **529**, 323 (1998); P. Ball,J. High Energy Phys. **01** 010 (1999).
- [50] V.V. Kiselev, A.K. Likhoded, and A.I. Onishchenko, Nucl. Phys. B **569**, 473 (2000); Phys. At. Nucl. **63**, 2123 (2000).
- [51] M.A. Ivanov, J.G. Korner, and P. Santorelli, Phys. Rev. D **63**, 074010 (2001).
- [52] W. Wang, Y.L. Shen and Cai-Dian Lü, Phys. Rev. D **79**, 054012 (2009).
- [53] T. Huang and F. Zuo, Eur. Phys. J. C **51**, 833 (2007).
- [54] R. Dhir, N. Sharma, and R. C. Verma, J. Phys. G **35**, 085002 (2008); R. Dhir and R. C. Verma, Phys. Rev. D **79**, 034004 (2009).
- [55] Junfeng Sun, Yueling Yang, Qin Chang and Gongru Lu, Phys Rev D **89**,114019 (2014).
- [56] C. H. Chang and Y. Q. Chen,Phys. Rev. D **49**, 3399 (1994).
- [57] V. V. Kiselev, A. E. Kovalsky, and A. K. Likhoded, Nucl. Phys.B **585**, 353 (2000); V. V. Kiselev, arXiv:hep-ph/0211021.

- [58] M. A. Ivanov, J. G. Korner and P. Santorelli, Phys. Rev. D **73**, 054024 (2006).
- [59] S. Naimuddin, S. Kar, M. Priyadarsini, N. Barik and P. C. Dash, Phys Rev D **86**,094028 (2012); S. Kar, P. C. Dash, M. Priyadarsini, S. Naimuddin and N. Barik Phys Rev D **88**, 094014 (2013).
- [60] P. Colangelo and F. De Fazio, Phys. Rev. D **61**, 034012 (2000).
- [61] A. Abd El-Hady, J. H. Munoz, and J. P. Vary, Phys. Rev. D **62**, 014019 (2000).
- [62] H. Fu, Y. Jiang, C. S. Kim, and G. L. Wang, J. High Energy Phys. **06** (2011) 015.
- [63] T. E. Browder and K. Honscheid, Prog. Part. Nucl. Phys. **35**, 81 (1995); M. Neubert, V. Rieckert, B. Stech, and Q. P. Xu, in Heavy Flavours, edited by A. J. Buras and H. Lindner (World Scientific, Singapore, 1992), and references therein.
- [64] A. Ali, J. G. Körner, G. Kramer and J. Willrodt, Z. Phys. C **1**, 269 (1979); J. G. Korner, and G. R. Goldstein, Phys. Lett. B **89**, 105 (1979).
- [65] H.-N. Li and S. Mishima, Phys Rev D **71**,054025 (2005).
- [66] Cai-Dian Lü, arXiv:hep-ph/0606094.